Technical report n°: AVI-NT-011-5242-CLS

Altimetric Mean Sea Surfaces and Gravity Anomaly maps Inter-Comparisons

Written by Fabrice Hernandez and P. Schaeffer

Preliminary version 3/05/2000

Contract CLS-CNES n° CLS/DOS/2125

TABLE OF CONTENTS

1 Introduction

Mean Sea Surfaces (hereafter called MSS) are by-products of satellite altimetry. Referenced to an Earth ellipsoid, they contain the geoid plus the dynamic ocean topography (hereafter called DOT). They are commonly used by geodesists and geophysicists to analyse geoid undulations, and studying crustal deformation, or Earth interior dynamics. Oceanographers using satellite altimetry can reference sea surface heights (hereafter called SSH) to the MSS. Due to the non perfect satellite positioning for repeat orbit missions, SSH are usually referenced to an MSS in order to reduce possible geoid cross-track artefacts. These are two reasons why a MSS is regularly associated to satellite altimetry products delivery.

By the way, to discuss the accuracy of MSS, it can be interesting to also analyse their Free Air Gravity Anomaly "companions". Because it is easier to focus on the shortest wavelength described by the gravity field, and second gravity anomaly surfaces (hereafter called GAS) can directly be compared to independent in-situ measurement of the Earth geopotential, that is marine gravity data. However, marine gravity data are not free from errors. Moreover, the shorter wavelength content of the gravity field –compared to the mean sea height signal– might be better estimated through a well tailored technique, which would not be adequate to estimate the larger wavelength content of the MSS.

Because the Jason-1 and Envisat altimetric satellite missions are scheduled in a near future, MSS and their GAS companions have to be proposed for supporting their respecting processing and product deliveries. Thus, the purpose of this note is to analyse the quality of several possible surface candidates already available in March 00, and propose a reasonable choice for the Jason-1 Science Working Team community. Both MSS and GAS are going to be compared, amongst the possible candidates, listed in Table 1. We will focus on three main points in these comparisons. The quality of the MSS along satellite tracks, in term of accuracy and wavelength content, which will affect the so-called "geoid cross-track correction". The global homogeneity of the surfaces, in order to quantify the capabilities in referencing simultaneously data from several satellite missions. And we will particularly verify known artefacts, like trackiness.

In collaboration with other teams, also analysing Jason-1 products, four MSS and Free Air Gravity Anomaly surfaces have been selected for the comparison study:

Mean Sea Surfaces	Free Air Gravity Anomaly Surfaces
CLS_SHOM98.2	*CLS_SHOM99*
GSFC00_MSS	*GSFC00_DG*
KMS_99_MSS	*KMS99*
OSU95	*no*
No	*Sandwell and Smith 97 (S&S97)*

Table 1: compared surfaces (on the same line if corresponding)

The three most recent products provide both MSS and the corresponding Free Air GAS. The OSU95 MSS and S&S97 GAS are included in these comparisons because they represent the standard products, regularly used by the whole community.

This paper is organised as follows: first, a presentation of the different surfaces is provided (note that the CLS_SHOM surfaces are particularly described here, since no reference publications have been issued yet); then the comparison/validation techniques are described in section 3. Sections 4 and 5 summarise the comparisons on MSS and GAS. Conclusions are given in section 6.

2 Surfaces description

The different MSS and free air GAS computed with altimetric data have been described below in order to give some hints for the comparison study. In section 2.6, Table 7 and Table 8 are summing up the main characteristics of the surfaces.

2.1 CLS_SHOM surfaces

2.1.1 Data processing

The CLS_SHOM98.2 has been estimated in order to provide a precise and high quality surface for oceanographic purposes. The first goal was to offer a SSH high precision along the T/P, ERS-1 and Geosat satellite repeat-orbit ground tracks. The second objective was to obtain an homogeneous reference. That is, a DOT content over the globe corresponding to a common averaging period, with the same kind of interannual oceanic processes, although the satellite data used where not collected at the same time. These two goals would aim to use the MSS as a referencing surface for near-real-time measurements provided by Jason-1, ENVisat or Geosat Follow On (GFO) satellites.

To fulfil these two requirements, Topex/Poseidon (T/P) data have been chosen to reference the MSS, but also to correct other set of altimetric data, because they provide the more precise measurements. The MSS estimation has also been designed in incorporating the two-year ERS-1 mean profile, the two-year Geosat mean profile, and the geodetic phase ERS-1 SSH. The geodetic data offer a finer spatial resolution at the vicinity of the ground tracks of the future satellite missions. To provide homogeneous data, the same type of altimetric corrections were applied to the four set of satellite measurements whenever possible.

First, the January 1993, to December 1995, SSH of T/P reprocessed Merged Geophysical Data Records (GDR-M Version C), distributed by AVISO (AVISO, 1996) were collected in order to compute the 3-year T/P mean profile. In the conventional way, SSH were corrected for tides (using the CSR3.0 tidal model, Eanes and Bettadpur, 1995), inverse barometer effects (local atmospheric pressure relative to a global pressure reference of 1013.3 mbar), sea state bias effects, tropospheric and ionospheric radar propagation perturbations. For more details on the corrections applied to T/P SSH data, the reader is referred to Le Traon and Ogor (1998). Then the mean profile was computed at each point of the ground tracks (approximately every 7 km) applying the conventional repeat-track analysis, by averaging the available SSH during the defined period (e.g., Cheney, 1983). Analysis at the cross-over points indicates a 1.7 cm rms height discrepancy (Table 3) which yield to an overall accuracy of about 1.2 cm (i.e. dividing the cross-over height discrepancies by $\sqrt{2}$, see Table 2).

Second, in order to compute the two-year ERS-1 mean profile, measurements from the two 35-day repeat missions were collected from the ocean products (OPRs) distributed by CERSAT (CERSAT, 1994; CERSAT, 1996). That is, cycles 7-17 (November 1992 to November 1993) of phase C, and cycles 2-12 (May 1995 to May 1996) of phase G. To obtain corrected SSH, data were processed in a similar way than T/P. Altimetric heights were referenced to the T/P ellipsoid instead of GRS80. The orbits calculated by DPAF (Deutsche Processing and Archiving Facilities) were used. Again, the other altimetric corrections are detailed in Le Traon and Ogor (1998).

ERS-1 geodetic data were also extracted from the OPRs distributed by CERSAT. The two geodetic mission non-repeat 168-day cycles (phases E and F) were processed as described above. These data span from April 1994 to March 1995. They are divided into nine 37-day and two 10-day subcycles.

As mentioned above, T/P SSH were used to improve the ERS-1 data accuracy. The ERS-1 DPAF orbits are less precise than T/P one, based on the JGM-3 gravity model (Tapley et al., 1996). Using the Le Traon and Ogor (1998) technique, large wavelength errors (typically orbit errors) can successfully be diminished. After the half-revolution spline adjustment, SSH cross-over discrepancies were reduced from 17 to 7 cm rms.

Then, T/P Sea Level Anomalies (SLA), witnessing the DOT variability, were also used to remove this variability in both the 35-day and the geodetic ERS-1 SSH. The technique, proposed by Hernandez (2000), interpolates T/P SLA on time and position of ERS-1 SSH. Correcting ERS-1 SSH with this estimation of the ocean variable signal 1) reduces the "ocean variability noise" caused by ERS-1 geodetic SSH incorporated in the MSS computation, 2) lowers the ocean seasonal variability aliasing while computing the mean profile using time-irregularly sampled data –which is the case by merging phase C and G ERS-1 SSH–, and 3) corrects the time averaged DOT provided by ERS-1 data to the three-year T/P time averaged DOT values. This last point contributes in incorporating in the MSS computation "homogeneous ocean content" data. A full description of these benefits is given in Hernandez (2000).

	T/P mean profile	ERS-1 mean profile	Geosat ERM mean profile	ERS-1 geodetic data
Time periods (date and satellite repeat cycles)	1993-94-95 cycles 11 to 121	11/92 - 11/93 7-17 phase C 05/95 - 05/96 2-12 phase G	11/86 - 11/88 cycles 1-44	04/94 - 09/94 phase E 10/94 - 03/95 phase F
Ground track spacing at the equator	315 km	~ 80 km	160 km	~ 8 km
Groundtracks number	254	1002	488	9644
Orbit inclination	66°	98°	108°	98°
North/South ground tracks limits (latitude)	66°	82°	72°	82°
Remarks	Used to reference other dataset	- merging 2 phases - DPAF orbit	- older dataset - less precise correction (e.g., wet tropo)	Finer spatial resolution
Specific processing		- ERS-1 individual profiles adjusted to T/P - Reduce DOT variability - Adjustment to the T/P mean profile	Adjustment to the T/P mean profile	- ERS-1 individual profiles adjusted to T/P - reduce DOT variability
Dataset accuracy (between 66°N et 66°S)	1.2 cm	1.6 cm	2 cm	6.5 cm
Dataset relative accuracy to T/P (between 66°N et 66°S)	1.2 cm	2 cm	3.2 cm	6.5 cm
Dataset relative accuracy to T/P for latitudes higher than 66°		4.8 cm	3.2 cm	10 cm

Table 2: summary of the dataset used for CLS_SHOM surfaces.
(Accuracy values are deduced from height discrepancies at crossover points).

Once corrected from the large wavelength errors, and from the "ocean variability noise", the ERS-1 geodetic SSH cross-over height discrepancies are reduced from 13 to 9 cm rms (Table 3). Thus, processed ERS-1 geodetic SSH offer a 6.5 cm accuracy (Table 2), assuming no-error correlations between ascending and descending tracks (i.e. dividing the cross-over height discrepancies by $\sqrt{2}$).

Two years (cycles 1-44) of the Geosat 17-day-repeat orbit Exact Repeat Mission (ERM) dataset were extracted from the NASA Ocean PathFinder Products, version 2, corresponding to the November 86 to November 88 period (Koblinsky et al., 1998). These products benefit from an orbit re-computation using the JGM-3 model. However, the other applied altimetric corrections are different from those used on T/P or ERS-1 data (for instance, tidal corrections are based on the SR960104 tidal model, see Schrama and Ray, 1994). Note also that the ocean variability reduction cannot be applied, because there was not any other altimetric satellite flying at that time. Less homogeneity with the other satellite dataset was thus expected from Geosat SSH.

The 2-year ERS-1 and Geosat mean profiles were then calculated. To reduce systematic biases, these two profiles were adjusted to the 3-year T/P mean profile at cross-over points by spline adjustment. After adjustment (Table 3), their accuracy is 1.6 and 2 cm rms respectively. Above 66° of latitude, that is, away from the T/P capabilities in correcting the other dataset, their accuracy drop to 4.8 and 3.2 cm rms respectively. In practice, in order to merge the data in computing the MSS, the relative discrepancies to the T/P mean profile are more useful, that is, 2 and 3.2 cm rms respectively.

	3-year T/P mean profile	2-year ERS-1 mean profile	2-year Geosat mean profile	ERS-1 geodetic data (*)
3-year T/P mean profile	1.66 (7904)	2.32 (62263)	3.45 (28591)	6.4 (112455)
2-year ERS-1 mean profile		2.97 (53576) 2.22 (43956) **		
2-year Geosat mean profile			2.8 (21583) 2.63 (20258) **	
ERS-1 geodetic data				9.2

Table 3: the four altimetric dataset: statistics of the crossover point discrepancies.
Standard deviations (cm rms) of ascending vs descending tracks of each type of satellite data, or between the ascending/descending tracks of the 3-year T/P mean profile and the other satellite dataset. The number of crossover points are indicated in brackets. (**) corresponds to statistics below 66° of latitude (to restrict the statistics to T/P area), and discrepancies lower than 30 cm (to eliminate crossover points near the coast). (*) two 37-day subcycles were used in the statistics.

In order to compute the free air gravity anomaly field, the DOT has to be removed from SSH, to provide "geoid" observations. This complementary processing was performed on the four set of altimetric data, by removing 1) the permanent tides, and 2) an estimate of the DOT provided by the dynamic height deduced from the Levitus '94 ocean climatology (see Levitus 1982, 1994a, 1994b).

2.1.2 Collocation technique

To compute the surfaces using the altimetric height as observations, a collocation technique has been implemented, based on a suboptimal inverse technique (e.g., Tarantola and Valette, 1982). The CLS_SHOM98.2 MSS and the CLS_SHOM99 Free Air GAS have been computed on a 1/16° (3.75') and 1/30° (2') grid respectively, oceanwide for latitudes below

±82°. There are two main benefits in using an inverse technique. First, multivariate estimation can be performed, that is, computing gravity anomaly using geoid observations. Second, observation budget errors can be considered and an a-posteriori estimation error field is provided by the optimal estimation theory. Note that by prescribing carefully the error budget, one set of data can be more or less weighted in the estimation formula.

The altimetric height budget error has been described by three terms. In a classical way, a noise value for each altimetric observation. More originally, the error due to the “ocean variability noise” mentioned above is also taken into account. It allows to restrain the impact of noisier ERS-1 geodetic data close to observations belonging to mean profiles. Finally, following the inverse technique proposed by Le Traon et al., (1998), altimetric along-track biases are considered. By introducing this last term, most of the biases caused by along-track errors beyond a 300-km wavelength limit might be reduced. In particular, biases caused by large scale oceanic interannual signal between Geosat SSH and the other set of data, or badly reduced orbit errors. In fact, by prescribing this long wavelength error, the “trackiness” artefacts usually seen in the surfaces are well reduced, as it would be assessed in section 4.

In practice, the estimation at each grid point of the surfaces is suboptimal. In other words, not the full dataset is used in the computation, but only a collection of relevant altimetric observations. Every observation of the mean profiles (the geodetic data) in a 30 (15) km radius are collected (respectively). Reducing the selecting radius of the dense geodetic dataset allows to decrease the time computation, without diminishing the estimate accuracy, since geodetic data are just used to provide the shortest scales around the estimation location. Then one observation over 10 is selected along-track in a 150 km radius. The second selection provides data constraints to control the long-wavelength error reductions. This procedure selects approximately at mid-latitude 300 observations, where 60 are comprised in the 30-km radius. Note that large scale structures of the geoid have been removed first to the data by subtracting the EGM96 geoid (Lemoine et al., 1996). After estimation, the EGM96 component is added back. Such remove/restore technique allow to focus the estimation on the shortest scales of the geoid. The final estimate corresponds to the full geoid spectrum although the high density selecting area is limited to 30 km. Note that in the case of the gravity anomaly computation, the geoid EGM96 is subtracted to the altimetric observations, then the gravity anomaly contribution of EGM96 is added back.

One of the key points of inverse optimal estimation is the use of prescribed covariance models, characterising the spatial statistics of the estimated field. In the case of the CLS_SHOM98.2 MSS determinations, we used homogeneously oceanwide the same correlation model, representing the mean sea height covariance. This model is isotropic, and has been adjusted along track to T/P and ERS-1 mean profiles, as:

$$\left\langle h(r_0)\cdot h(r_0+r)\right\rangle = \mathrm{var}(h)\left[1+r+\frac{r^2}{6}-\frac{r^3}{6}\right]\exp(-r)$$

where $r=\sqrt{x^2+y^2}\,/12$ is proportional to the distance between two altimetric height points, and $\mathrm{var}(h)$ is the local variance of the height observations. This model is characterised by a ~40-km zero crossing, and a small negative lobe.

In the case of the gravity anomaly determination, a set of other specific functions were chosen. In fact, for the Earth gravity field, and its derived fields –the geoid or the gravity anomaly– a family of covariance models can be defined (e.g., Forsberg, 1987 ; Meier, 1981). A set of third order Markov functions (Jordan, 1972) have been chosen and fitted empirically to the altimetric heights relative to EGM96. Cross validations were carried out to check the reliability between this set of functions and the MSS covariance model described above. Then empirical adjustment have been proceeded in each suboptimal box, in order to parameterise either the variance and the zero crossing in each box. The zero crossing values are plotted in Figure 1. This figure shows that typical scales of the gravity field are shorter near the oceanic ridges, than in the middle of abyssal plains. Thus by using “tuned” covariance models in each suboptimal box, it allow us to better take into account the shortest scales of the marine gravity field.

In order to validate these choices of covariance models in both the MSS and the GAS estimation method, robustness tests were performed to ensure the consistency between errors on the estimates, and the estimation error field provided by these methods, which depends drastically on these models. In practice, for the GAS determination, the zero crossing of the variable covariance models were restricted to 25-75 km. Such limitations ensure to reduce short scale noise when the zero crossing radius is smaller, and to control estimate smoothing when it is too large.

Finally, near the coast, some specific procedures had to be developed. In fact, due to the inaccuracy or lack of satellite data, the grid point computation near the coast is either inaccurate or not performed. However, the MSS and Free Air GAS grids are often used through interpolations. And any interpolating scheme needs some grid points around. It is thus necessary to provide surfaces with some continuity toward the continents. For the CLS_SHOM98.2 MSS, computation was limited to ocean depth greater than 10 meters. Then an extrapolating scheme conserving the gradients was applied over a 100-km band inside the continent. In the case of the marine gravity determination, the method was refined, by directly using the inverse estimation technique. For grid points over continent, the correlation models were extended up to 150 km, in order to select more distant valid altimetric observations. In both case, the a-posteriori estimation error field is witnessing these specific extrapolations, in order to use these grid points only as “continuity values” for interpolation schemes, rather than as confident deep ocean estimates.

Let’s remarks before closing this description that the quality of the surface is not homogeneous oceanwide. At latitude greater than 66°, there is no more T/P data: first the estimate would be less precise, and second, because ERS-1 data can not be corrected, the influence of the "ocean noise variability” increases. These effects would be amplified again beyond 72° of latitude, where only ERS-1 data are available. Note also that the spatial data density augments poleward.

2.2 GSFC surfaces

The Goddard Space Flight Center (GSFC) recent products were just released, and no reference paper has been published yet. The previous version, the GSFC98 MSS is described in Wang (2000) but the determination technique developed for this new MSS is different. The description given below is directly copied from their web site (magus.stx.com, Y.M. Wang, personal communication). The GSFC00_MSS is the mean sea surface computed from the following satellite altimeter data: T/P, ERS-1 and ERS-2, and Geosat. Both the geodetic data from Geosat and ERS-1 are incorporated in the estimation procedure. The GSFC00_DG is the altimetry GAS directly computed from the mean sea surface GSFC00_MSS.

Both the MSS and the GAS were computed on a 2' grid oceanwide between latitude ±80°. The larger set of altimetric data has been incorporated in these surfaces calculations (see Table 4). A six-year T/P mean profile has been computed, using T/P data from cycles 11 to 232 (January 93 – December 98). Geosat ERM cycles 1-42 were used to compute an almost 2-year mean profile. A multi-year ERS-1 and ERS-2 35-day repeat cycles has also been computed, using ERS-1 Phase C: Cycles 1 to 18; Phase G: Cycle 1 to 13; and ERS-2: Cycle 1 to 29). New environmental corrections were also applied to the Geosat Geodetic Mission

(GM) data and the ERS-1 168 day data (Koblinsky et al., 1998). Note that through the Ocean Pathfinder Project, a particular effort has been done in using homogeneous type of altimetric corrections. Tidal corrections are based on the SR960104 model (see Shum et al., 1997), and satellites orbits were all based on the JGM-3 model (Tapley et al., 1996) –the ERS-1 DGM-E04 orbits are JGM-3 based orbits calculated by the Delft Institute of Technology–

The mean sea surface height along the oceanic study dedicated missions (T/P, Geosat ERM and ERS-1/2 35 day repeat missions) were averaged into mean profiles. The 6-year T/P mean profile is used to reference the surfaces. That is, the two other satellite mean profiles were adjusted to the TOPEX mean in 2° (0.5° border) latitude bands.

	T/P mean profile	ERS-1/2 mean profile	Geosat ERM mean profile	Geosat GM data	ERS-1 geodetic data
Time periods (date and satellite repeat cycles)	1993-98 cycles 11 to 232	1991-97 1-18 phase C 1-13 phase G 1-29 ERS-2	11/86 - 10/88 cycles 1-42	March 1985 – October 1986	04/94 - 09/94 phase E 10/94 - 03/95 phase F
Ground track spacing at the equator	315 km	~ 80 km	160 km	~4 km	~ 8 km
Groundtracks number	254	1002	488	~8000	~9500
Orbit inclination	66°	98°	108°	108°	98°
North/South ground tracks limits (latitude)	66°	82°	72°	72°	82°
Remarks	Used to reference other dataset	- merging 3 phases - DGM-E04 orbits	- older dataset - less precise corrections	- older dataset - finer spatial resolution - less precise corrections	Fine spatial resolution
Specific processing		Mean profile adjustment to T/P mean profile by 2° latitude bands	Mean profile adjustment to T/P mean profile by 2° latitude bands	Along-track gradients used instead of heights, to reduce variability errors	Along-track gradients used instead of heights, to reduce variability errors

Table 4: summary of the dataset used for GSFC surfaces.

The MSS gridding procedure (i.e., the collocation technique) is based on a 2-dimensional Fourier series in 2° by 2° cells (1° by 1° predication area plus 0.5° border). An a-priori observation error was prescribed to 2, 4, and 4 cm for T/P, ERS-1/2 and Geosat respectively. The Nyquist frequency was 1/11', which is corresponding to a spatial resolution of 21 km at the equator. To take into account “ocean variability noise” causing trackiness on the estimated surface, geodetic data (Geosat GM and ERS-1 168-day) were incorporated in the estimation procedure as along track SSH gradient instead of classically the sea surface height. Thus, observation of adjusted mean sea surface heights, including the mean sea surface height of the 6–year T/P mean profile, were combined with observations of sea surface height slopes of the two geodetic missions during the determination of the 2D Fourier series. To stabilise the solution, a priori degree variance were adopted and the 2D Fourier coefficients were determined in such a way that the root mean squares of the differences of the sea surface height and the sea surface height slope differences were minimum. The a-posteriori

estimation error field of the GSFC00 mean sea surface height has also been provided for each 2' cells.
The free Air Gravity Anomaly field (GSFC00_DG) was computed by applying the inverse Stokes integral to the mean sea surface heights implied geoid undulations. No a-posteriori estimation error is provided.

2.3 KMS surfaces

2.3.1 The KMS99 Free Air Gravity Anomaly surface

This is a recent surface, released in March 2000, which has no published reference yet. This is an upgraded version of the KMS98 altimetric gravity field, described in Andersen and Knudsen (1998), Knudsen and Andersen (1998), and Knudsen and Andersen (1997). Traditionally, the KMS products were focusing on recovering the marine gravity signal, by constraining essentially their determinations with the dedicated Geosat and ERS-1 satellites geodetic missions. They have introduced in their new computation the T/P and ERS-1 (35-day repeat data) mean profiles (see Table 5).

A 5-year T/P mean profile has been calculated using data from the first 150 cycles (September 92 to September 96). The 18 cycles of the ERS-1 phase C (April 92 to December 93) were also processed to compute a mean profile. Geodetic data from the 18 months of the Geosat GM, and from the two 168-day ERS-1 geodetic cycles were collected. All the altimetric heights were referenced to a JGM-3 orbit. Tidal corrections were based on the AG95.1 model (Andersen et al., 1995).

To reduce orbit errors, altimetric corrections errors, and biases between satellite tracks due to different interannual, seasonal, and mesoscale DOT content (data span from 1985 to 1996), altimetric heights were processed by cells of 3° in latitude to 12° in longitude. SSH were adjusted along-track to a geoid model by removing a tilt and a bias. The EGM96 geoid has been used world-wide, except in Arctic areas where a local tailored geoid was available. Then a weighted crossover track minimisation was performed.

	T/P mean profile	ERS-1 mean profile	Geosat GM data	ERS-1 geodetic data
Time periods (date and satellite repeat cycles)	1992-96 cycles 2 to 150	1991-93 1-18 phase C	March 1985 – October 1986	04/94 - 09/94 phase E 10/94 - 03/95 phase F
Ground track spacing at the equator	315 km	~ 80 km	~4 km	~ 8 km
Groundtracks number	254	1002	~8000	~9500
Orbit inclination	66°	98°	108°	98°
North/South ground tracks limits (latitude)	66°	82°	72°	82°
Specific processing	Adjustment in 3° lat x 12° lon cells to reduce orbit errors and DOT components. Along-track removal of bias and tilt to SSH relative to EGM96. Then crossover point minimisation between arcs.			

Table 5: summary of the dataset used for KMS surfaces.

A first 1/16° gridding of the adjusted height was performed, by cells of 4° (lat) by 16° (lon), with a border of 1° by 3°. The gridding procedure was based upon a local least square collocation technique (i.e., an inverse technique), using the 48 nearest observations. A second-order Markov SSH covariance function was prescribed. However an along-track correlated noise term was added to the covariance error matrix, to reduce biases between tracks. Note that prior any inversion, the local mean height, calculated over the nearest 100 observations by a weighted averaging, was removed to the data, to ensure a better reduction of the DOT residual signal.

Then the GAS was calculated in 2 (±0.5)° latitude by 10 (±1)° longitude cells, from the gridded mean sea height field. A 2-D FFT procedure was carried out to obtain sea height harmonics, then compute the gravity anomaly harmonics, and determine from it the free air gravity anomaly surface. Note that a low-pass filter –corresponding to a 12-km cut-off– was applied on the gravity Fourier harmonics to reduce short wavelength noise. To obtain the full signal, the EGM96 gravity anomaly field was restored.

In practice, the mean sea height gridding procedure and the FFT estimations were proceeded using the GRAVSOFT package (Tscherning et al., 1992).

2.3.2 The KMS99 Mean Sea Surface

This is also a brand new product, delivered early this year, and which has no published reference yet. This is an upgraded version of the KMS98 MSS, described in Knudsen and Andersen (1998). This MSS is determined on a 1/16° grid (3.75').

The KMS99_MSS is partly deduced from the KMS99 gravity anomaly field. Using the non-filtered 2-FFT gravity harmonics (see 2.3.1), the short wavelength of the mean sea height were recovered. To obtain wavelength longer than 1000 km, and also the DOT content, a first guess of global spherical harmonics were adjusted to the 5-year T/P mean profile. Then spherical harmonics deduced from the 1.7-year ERS-1 mean profile were adjusted to this guess. Finally, the 2-FFT gravity harmonics were combined to this spherical harmonics solution expended only to degree and order 20, to provide a full spectrum MSS.

2.4 The OSU95 MSS

The Ohio State University mean sea surface is the oldest in our comparisons, but it is interesting to refer to it because it has been widely used in the satellite altimetry community. The OSU95 MSS has also widely used in comparison studies with other surfaces (e.g., Wang, 2000). Information concerning this surface were gathered in Yi (1995) and Rapp (1998).

The surface was determined using (see Table 6) one-year mean profiles: of TOPEX only ; of the first year of Geosat ERM data ; and of the 35-day repeat ERS-1 IGDR (Intermediate Geophysical Data Records). High spatial resolution was provided by the IGDR of the first ERS-1 geodetic 168-day cycle. Orbits were computed using the JGM-2 model (Nerem et al., 1994), and altimetric heights referenced to the T/P ellipsoid. Tide corrections were based on the Cartwright and Ray (1990) model, improved by 1.5 year of T/P data. To reduce ERS-1 orbit errors, the cycles of the 35-day repeat ERS-1 IGDR were adjusted at crossover to T/P GDR. Once the one-year mean profiles were computed, the ERS-1 and the Geosat profiles, but also ERS-1 geodetic individual tracks were adjusted to the T/P mean profile in cells of 25 ±5° of latitude by 190 ±5° of longitude, by removing tilt and biases.

The MSS determination, on a 1/16° grid, oceanwide from 80°S to 82°N, was based on a local least square minimisation collocation technique. First, a geoid model was removed to the altimetric heights. A tailored geoid model based on the degree-360 OSU91A model (Rapp and Pavlis, 1990 ; Rapp et al., 1991) combined with the spherical harmonic model of JGM-3 coefficients up to degree and order 70 was used. Then for each grid point, data in a radius of 70 km were gathered, in order to finally select 20 observations in each quadrant. A noise level of 2, 5, 4, and 10 cm was prescribed to TOPEX, ERS-1, Geosat, ERS-1 GM SSH respectively. Then the local inverse estimation was carried out using a second-order Markov covariance model, with a correlation length of 70 km. The final MSS was obtained by adding back the tailored geoid model.

	TOPEX mean profile	ERS-1 mean profile	Geosat ERM mean profile	ERS-1 geodetic data
Time periods (date and satellite repeat cycles)	02/93 - 03/94 cycles 17 to 53	11/92 - 11/93 7-17 phase C	11/86 - 11/87 cycles 1-22	04/94 - 09/94 phase E
Ground track spacing at the equator	315 km	~ 80 km	160 km	~ 8 km
Groundtracks number	254	1002	488	4822
Orbit inclination	66°	98°	108°	98°
North/South ground tracks limits (latitude)	66°	82°	72°	82°
Remarks	Used to reference other dataset	- JGM-3 orbits - IGDR data	- JGM-3 orbits - less precise correction (e.g., wet tropo)	- Finer spatial resolution - IGDR data
Specific processing		- ERS-1 individual profiles adjusted to T/P - Adjustment to the TOPEX mean profile	Adjustment to the TOPEX mean profile	- ERS-1 individual profiles adjusted to T/P - Adjustment to the TOPEX mean profile

Table 6: summary of the dataset used for the OSU95 Mean Sea Surface.

2.5 The Sandwell and Smith 97 Free Air Gravity Anomaly surface

This GAS, will be the reference of our comparison work. The following description is based on the Sandwell and Smith (1997) article.

The gravity anomaly surface is first built on geodetic satellite altimetry: ERS-1 and Geosat GM, providing a short wavelength description of the earth geopotential. The 35-day ERS-1 SSH and 17-day repeat Geosat ERM were also included as mean values (or more precisely, “stacked” values). The orbits of the different set of altimetric data were computed using the JGM-3 model (Tapley et al., 1996). The CSR3.0 tidal model (Eanes and Bettadpur, 1995), was also systematically used for correcting altimetric heights. Most of the other classical altimetric corrections, just as DOT biases or altimetric biases between the different dataset were of less importance since SSH along-track slope was the base of the estimation procedure. Notice that –as usual to remove geopotential long wavelength– a geoid model based on JGM3 spherical harmonics up to degree 60 was removed to the SSH. Then an along track low-pass filter with a ~20km cut-off was applied to reduce altimetric noise. Instead of calculating mean profiles from ERS-1 and Geosat repeat mission dataset, a stacking was used to build stacked profiles.

The estimation procedure is far different from classical methods. Along-track SSH slopes were calculated. Then a binning in 2’ cells was carried out separately on each set of slopes altimetric data. The binned value corresponded to the result of a median filtering over all the data available in the bin. Empty bins were filled using adjacent valid bins by performing a distance-weighting interpolation. Then a merging of the different binned surfaces was performed. From the merged binned map, east and north components of the vertical deflections were globally calculated by differentiation. This procedure was performed iteratively to remove spurious data. Then, 2D-FFT of the vertical deflections was computed. From the two sets of harmonics, the gravity anomaly harmonics were determined. Then an inverse Fourier transform was applied to provide a gravity anomaly map with a 2' resolution. The long wavelengths were restored by adding back the gravity anomaly contribution of the geoid model previously removed.

2.6 Summary

The main characteristics of the four MSS are:

	CLS_SHOM98.2	**GSFC00_MSS**	**KMS99_MSS**	**OSU95**
Geographical characteristics	1/16° (3.75') oceanwide ±82° latitude	1/30°, shifted 1/60° (2') oceanwide ±80° latitude	1/16° (3.75') oceanwide ±80° latitude	1/16° (3.75') oceanwide 80°S-82°N latitude
Reference ellipsoid	T/P	T/P	T/P	T/P
Data used	- 3-year T/P mean profile - 2-year ERS-1 mean profile - 2-year Geosat mean profile - 2 168-day ERS-1 geodetic cycles	- 6-year T/P mean profile - 5.7-year ERS-1/2 mean profile - ~2-year Geosat mean profile - 2 168-day ERS-1 geodetic cycles - Geosat geodetic data	- 2-FFT of the gravity anomaly field - Spherical harmonics to degree and order 20 adjusted to the T/P and ERS-1 mean profiles.	- 1-year T/P mean profile - 1-year ERS-1 mean profile - 1-year Geosat mean profile - 1 168-day ERS-1 geodetic cycles
Estimation technique	Suboptimal inverse technique	Spectral estimation (2D Fourier series)	Spectral estimation (2D Fourier series)	Suboptimal inverse technique
A-posteriori estimation error field	Yes	Yes	No	No

Table 7: Mean Sea Surface characteristics summary.

The main characteristics of the four free air gravity anomaly fields are:

	CLS_SHOM99	**GSFC00_DG**	**KMS99**	**Sandwell & Smith 97**
Geographical characteristics	1/30° (2') oceanwide ±82° latitude	1/30°, shifted 1/60° (2') oceanwide ±80° latitude	1/30° (2') oceanwide ±80° latitude	1/30° (2') oceanwide ±80° latitude
Reference ellipsoid	T/P	T/P	T/P	T/P
Data used	- 3-year T/P mean profile - 2-year ERS-1 mean profile - 2-year Geosat mean profile - 2 168-day ERS-1 geodetic cycles	GSFC00_MSS	- 5-year T/P mean profile - 1.7-year ERS-1 mean profile - 2 168-day ERS-1 geodetic cycles - Geosat geodetic data	- Geosat ERM - ERS-1 35-day - Geosat GM - ERS-1 GM
Estimation technique	Multivariate suboptimal inverse technique	Inverse Stokes integral of the MSS	Spectral estimation (2D Fourier series)	Vertical deflection binning Spectral estimation of the VD, then gravity anomalies
A-posteriori estimation error field	Yes	No	Yes	No

Table 8: Free Air Gravity Anomaly Surface characteristics summary

3 Comparison methods

As we already mentioned, the interest of a MSS or a GAS is not only the field accuracy at each single grid point, but much more the overall precision on a wider range of wavelengths.

Because MSS will be more and more devoted to reference at a glance altimetric measurements originated from several satellites, it is important to assess its oceanwide homogeneity. Heterogeneity of the surfaces might be caused by several factors. First, different DOT content of the satellite data incorporated into the surface determination, typically heights from mean profile averaged over different periods, or from geodetic missions, contaminated by "ocean variability noise". Second, difference in the geoid wavelength content of the data, due to distinct or inadequate altimetric data filtering. Third, regionally differences on the estimation procedure, due to the variable coverage of satellite data –in particular in polar areas– or weighting of the data.

Further than these points, because the determination of the gravity anomaly tend to amplify short wavelength noise, it is interesting to focus on the GAS shortest scales to assess their accuracy.

Therefore, our comparisons will concentrate on:

- Analyse the height differences between the MSS and the altimetric mean SSH profiles. Assuming that a mean profile is more accurate than an MSS. We will use the 3-year T/P, the 2-year Geosat, and the 2-year ERS-1 mean profiles computed at CLS and used in the CLS_SHOM98.2 determination. This is not –obviously– an independent comparison. However, these profiles were carefully analysed, and their accuracy is almost known (see Table 3). Note that these profiles have been adjusted in term of DOT content, that is, the 2-year ERS-1 mean profile oceanic signal should be close to the 3-year T/P mean profile oceanic information (Hernandez, 2000). These along track analysis would be carried out in two ways. First by looking at height differences between the altimetric profiles and the MSS, to infer quantitatively the MSS height "precision". Second by analysing the along-track slope differences, to study the short wavelength content of each MSS, at location where they are the most precise (which means that elsewhere, precision should be worse).
- Analyse the differences between the four MSS surfaces. Quantitatively, it allows to see similarities between the different products. Qualitatively, it is particularly useful for detecting specific artefacts: trackiness, large discrepancies due to interannual oceanic oscillations, oceanic mesoscale noise, or noise along the coast.
- Analyse the differences between the four GAS surfaces. It might reveal systematic biases due to estimation procedure used (all are differentiations of height to gravity, which might raise a "constant" problem). And then, at short wavelengths more or less pronounced noise.
- Analyse the differences between the four GAS, and marine gravity measurements. This is the only "true" independent comparisons, commonly carried out (e.g., Sandwell and Smith, 1997 ; Andersen and Knudsen, 1998). But it has to be carefully applied since marine gravity data are not cleared of errors. These comparisons might help to infer the short wavelength precision of each surface.

Note that the surfaces display different grid spacing (see Table 7 and Table 8). To homogenise our comparisons, all the grids were re-interpolated on a 1/16° for MSS, and 1/30° for GAS. The same bi-cubic interpolating scheme was used in all cases.

4 Mean Sea Surfaces comparisons

4.1 Along-track comparisons

The four MSS were compared to the three SSH mean profiles computed at CLS (see Table 3). Similar comparisons were performed by Wang (2000) on the GSFC98 MSS, with their 6-year T/P and 3-year ERS-2 mean profiles.

	T/P			ERS-1			Geosat		
	Mean height dif.	St. Dev. height dif.	St. Dev. slopes dif.	Mean height dif.	St. Dev. height dif.	St. Dev. slopes dif.	Mean height dif.	St. Dev. height dif.	St. Dev. slopes dif.
GSFC00	-0.09	2.19	0.12	-0.05	3.36	0.23	-0.12	3.80	0.20
CLS_SHOM98.2	-0.13	1.22	0.09	-0.17	1.94	0.14	-0.25	3.85	0.13
OSU95	0.40	3.54	0.14	0.14	5.16	0.28	0.25	4.47	0.26
KMS99	-0.40	6.18	0.32	-0.55	7.58	0.36	-0.13	7.29	0.37

Table 9: Statistics of the along-track differences between MSS and altimetric mean profiles. Mean and standard deviations of the height differences are in cm. Standard deviations of the along-track slopes differences are in cm/km. Height differences exceeding 50 cm were excluded. The along-track height differences were calculated between 80°S and 80°N.

Mean sea height differences between mean profiles and MSS were computed by interpolating the grids at the mean profile along-track positions. Then along-track slopes were computed using successive along track points. Global illustrations of these differences are given by the along-track height differences between the 3-year T/P mean profile and the four MSS in Figure 2 and Figure 3.

Height difference statistics are witnessing: 1) distinct DOT contents in the mean profiles and the MSS ; 2) possible systematic biases (e.g., different altimetric correction and orbit models); and 3) respective precision of the mean profiles and the MSS. Table 9 shows that the KMS99 and the OSU95 MSS are out-ranging the comparisons with the mean profiles, whereas the GSFC00 and CLS_SHOM98.2 surfaces are rather close. The OSU95, CLS_SHOM98.2 and GSFC00 MSS were first computed for referencing satellite altimetry, while the KMS99_MSS is a by-product of a GAS, based essentially on geodetic dataset. In particular, the ERS-1 and T/P mean profiles were added to constrain the KMS99 MSS long wavelengths. It is thus not surprising to observe larger discrepancies along the mean profiles. The OSU95 MSS has been determined with less accurate dataset, in particular the ERS-1 Intermediate GDR products which explains the stronger differences. This is clearly illustrated by Figure 2, where we detect: 1) patchy differences associated with strong variable oceanic areas (western boundary currents, Antarctic Circumpolar Current) ; 2) large scale differences appear in the Tropics (due to interannual changes of the tropical DOT pattern) ; and 3) basin scale shifts (possibly caused by geographically correlated altimetric errors).

Height difference standard deviations show that the CLS_SHOM98.2 MSS is closer to the T/P and ERS-1 mean profiles than the GSFC00 MSS. This is partly explained because 1) we compare the CLS_SHOM98.2 MSS with the profiles incorporated in its determination and 2) because these mean profiles correspond to a DOT averaging over 1993-95, while the GSFC00 MSS is based on a 6-year and 5-year averaged DOT along T/P and ERS respectively. The global distributions of these discrepancies are shown in Figure 3: The height differences between the 3-year T/P mean profile and the CLS_SHOM98.2 MSS –rather small– are located at the vicinity of semi-enclosed seas, or in high oceanic variability areas. While larger differences appears with the GSFC00 MSS. Large scale differences in the Tropics might be caused by differences in DOT averaging between the 3-year and the 6-year period, in particular because there was an El Nino event in 1997.

However, patchy differences with values exceeding 3 cm are observed in every large oceanic variability area. It means that either the 3-year T/P mean profile is noisy (contaminated by the ocean variability) compared to the 6-year T/P mean profile included in the GSFC00 MSS ; or both the 3-year and 6-year profiles are accurate, but the GSFC00 MSS is contaminated by "ocean variability noised" SSH, like geodetic mission data. A careful look of T/P mean profiles accuracy suggest that the second assumption is more realistic. Hernandez (2000) shows that from a 3-year to a 5-year T/P mean profile, the crossover discrepancy statistics decrease from 1.66 to 1.58 cm rms, which means that the 3-year mean profile is already accurate. Moreover, Wang (2000) indicates that the GSFC00 6-year mean profile is characterised by crossover discrepancy statistics of 1.9 cm rms. Which means that the 3-year T/P mean profile we use here is as accurate or better than the GSFC00 6-year T/P mean profile.

There is a gap between the height differences with ERS-1 regarding the one of T/P in the case of the CLS_SHOM98.2 MSS, and in the case of the GSFC00 MSS. It could reflect a better DOT content homogeneity in the CLS_SHOM98.2 MSS. Table 3 shows that the T/P and ERS-1 mean profiles are ~1.2 cm and ~1.6 cm accurate respectively. Assuming MSS determination errors globally similar, the lag in T/P versus ERS-1 discrepancies, different in the GSFC00 and CLS_SHOM98.2 comparisons is witnessing a less DOT homogeneous content in the GSFC00 MSS.

Following the same considerations, height differences of these two MSS with the 2-year Geosat mean profile are rather close, because both surfaces seems to have incorporated the DOT content associated with the Geosat period (1986-87). Note that in both estimations, less confidence was given to Geosat observations, and thus, even along Geosat groundtracks, the MSS are still influenced by other satellite dataset. This is well illustrated in the Ionian and Aegean basins, where Geosat groundtracks exhibit large differences with the MSS while neighbouring T/P groundtracks are comparable to the CLS_SHOM98.2 (Figure 4). Note that in the case of the GSFC00 MSS, large differences are observed in the Alboran sea and the Levantine basin (Figure 5). These discrepancies may be due to 1) different DOT content between the GSFC00 MSS and the mean profiles we are using, or 2) the satellite tracks incorporated in the GSFC00 MSS were badly adjusted, due to the rather irregular shape of these basins.

Slope differences are smaller for the CLS_SHOM98.2 MSS than for the other surfaces. This is not surprising, since a filtering with a 12 to 20 km cut-off has been applied on the SSH prior any MSS determination, except in the case of the CLS_SHOM98.2 surface. Moreover, let's remind that these mean profiles, containing SSH wavelengths of the order of 7-10 km were incorporated in the CLS_SHOM98.2 MSS. However, because a MSS results from a local merging of surrounding data, it is satisfactory to observe than MSS gradients along "good" tracks like the T/P and ERS-1 mean profiles are not contaminated by noisier geodetic data.

4.2 Grid to grid comparisons

Grid comparisons allow to figure out which wavelength, or which noise are present in the different MSS, and of course, which are their DOT content. We have first examined separately the four MSS relative to EGM96, in order to focus on the shortest scales, looking for "visible" artefacts. Figure 6 and Figure 7 show examples in the Pacific ocean. The OSU95 MSS offer a rather poor description compared to the others: The trackiness effects appear clearly along Geosat or ERS-1 tracks ; and the Ridge is smooth and not well represented. The

KMS99 MSS better represents the fine structures of the ocean floor. However, the trackiness effects along Geosat or ERS-1 GM tracks are still contaminating the surface.

The GSFC00 and CLS_SHOM98.2 MSS give a sharper description of the geoid undulations. Although, some trackiness effects are still present in the GSFC00 surface. It seems that taking into account along-track errors in the CLS_SHOM98.2 MSS determination strongly reduced these artefacts. Short wavelength are better represented in the CLS_SHOM98.2 MSS, which corroborates the statistics of the along-track height slope differences (see Table 9). However, over "flat bottom areas", both the CLS_SHOM98.2 and the GSFC00 MSS are clearly exhibiting the so-called "orange skin" effect, which corresponds to short scales noise.

Grid differences	All points	Differences < 50 cm (*)	Points below lat. 66° (**)
CLS_SHOM98.2 - GSFC00	-2.6 ± 8.6 (9565819)	0.0 ± 5.6 (9479045)	0.1 ± 6.0 (8750839)
GSFC00 – OSU95	0.4 ± 9.5 (9586145)	0.3 ± 7.6 (9516341)	0.3 ± 7.3 (8753670)
GSFC00 – KMS99	-2.3 ± 17.1 (9964929)	-0.8 ± 9.7 (9557264)	0.1 ± 8.5 (8833308)
CLS_SHOM98.2 – KMS99	-1.9 ± 14.3 (9519494)	-0.6 ± 8.9 (9268515)	0.1 ± 8.0 (8749894)
KMS99 – OSU95	2. ± 14.7 (9507091)	0.9 ± 9.7 (9260962)	0.3 ± 9.2 (8750055)
CLS_SHOM98.2 – OSU95	0. ± 10.2 (9603934)	0.2 ± 7.8 (9507269)	0.5 ± 7.8 (8755410)

Table 10: Statistics of the four MSS grid differences (in cm) between 80°S and 80°N. The first value is the mean difference. The second values is the standard deviation of the differences. The bracketed number corresponds to the number of differences. (*) Height differences exceeding 50 cm were excluded. (**) Excluding points at higher latitudes than 66°.

The differences between the GSFC00 or the CLS_SHOM98.2 MSS with the "old" OSU95 MSS (see Figure 9 and Figure 13) reveal the OSU95 inaccuracy, in particular, strong trackiness effects are visible. Then, changes in Tropical ocean signals, that exceed 10 cm, also cause differences. Note that these Tropical height differences are quite similar to what was observed in the comparisons with the 3-year T/P mean profile (Figure 2). Finally large discrepancies in the high oceanic variability area are visible. As we already mentioned, this is due to the poor quality of the altimetric data used to determined the OSU95 MSS, and also to their different DOT content.

The closest surfaces are the GSFC00 and the CLS_SHOM98.2 MSS (Figure 8). Table 10 shows that discrepancies are of the order of 5.7 cm rms, and they present similar difference level with the OSU95 MSS. GSFC00 and CLS_SHOM98.2 MSS differences correspond first to large scale DOT differences of the order of 4-6 cm rms, as it can be seen in the Tropics. Second, strong differences, larger than 10 cm, appears in the high oceanic variability areas. Third, in the Arctic and Antarctic areas differences exceeding 10 cm are noticeable. A step in latitude is also observed at 70°N in the Atlantic ocean between the GSFC00 and CLS_SHOM98.2 MSS as shown by Figure 14. This step also appears in the grid differences between the GSFC00 and the OSU95 MSS, but not between the OSU95 and the CLS_SHOM98.2 MSS, which tend to prove that some artefact is contaminating the GSFC00 MSS in this area.

The comparisons between the KMS99 and the other MSS present the largest differences: Table 10 shows discrepancies of 10 cm rms, or larger, and the mean differences are not negligible. Part of it are due to comparisons at high latitudes, where the KMS99 level is higher (see Figure 10 and Figure 11). However, if differences are not observed in the tropical band, large discrepancies of more than 10 cm appear elsewhere in the energetic oceanic areas. This might be due to a lower accuracy of the surface at wavelength between 100 km and 1000 km.

5 Free Air Gravity Anomaly surfaces comparisons

To first illustrate the GAS accuracy, let's first examine the profiles of the four GAS, along the 347°E longitude, between 20-30°S, in Figure 15. The KMS99 GAS is the smoothest, and CLS_SHOM99 the sharpest. This is verified by the statistics of each profile in Table 11. Nevertheless, analysing qualitatively the different features present in each profile, the S&S97, the GSFC00 and the CLS_SHOM99 GAS seem to provide alternatively precise descriptions, and it is difficult to assess whether one or the other is more accurate. Is thus necessary to obtain independent measurements of the gravity field, like marine gravity data, and analyse the GAS relative to these data.

Grids	Mean value (mgal)	Standard deviation (mgal)
GSFC00	5.2	16.7
CLS_SHOM99	5.4	18.3
KMS99	4.3	16.9
S&S97	5.0	18.1

Table 11: Statistics of the four GAS profiles along 347°E.

This is the reason why we chose to compare the four GAS in specific areas, in order to focus on the shortest wavelength. Three sets of marine gravity data were available to us, with different levels of accuracy. These three dataset are characterised by different spatial resolutions, they thus offer distinct sampling of the gravity field. Therefore, the comparisons were performed in the three corresponding areas, that is, in the North Atlantic, in the South Atlantic, and South of Japan, as illustrated by Figure 16.

The CLS_SHOM99 is not incorporating Geosat GM data, which are noisy, but which provide the shortest geoid scales. These shortest scales are the keypoint of the GAS estimations: altimetric height noises are amplified, and the GAS determination is a compromise between data noise and short wavelength filtering. In the case of optimal inverse methods, the prescribed covariance models play a significant role. Thus, several complementary comparisons were carried out in the North Atlantic area, with alternative determinations of the CLS_SHOM GAS (where the covariance models were modified).

5.1 The South Japan area

A large set of marine gravity data, provided by the BGI (Bureau Gravimétrique International) were extracted in the 125-145°E / 24-35°N area. It is a "low accuracy" marine dataset. The 507768 measurements are not cross-validated, and we detected sometimes 10 mgal gaps between legs. However, we decide to perform comparison with this set of measurements simply to obtain a first guess on GAS relative accuracy.

Grids	All the data	Removing diff. > 50 mgal
GSFC00	-3.0 ± 12.0	-3.2 ± 9.8 (6283)
CLS_SHOM99	-3.3 ± 12.9	-3.3 ± 10.8 (6506)
KMS99	-3.3 ± 12.4	-3.4 ± 10.0 (6409)
S&S97	-3.1 ± 12.1	-3.0 ± 11.0 (5965)

Table 12: Statistics of the differences between the marine gravity measurements in the South Japan area and the corresponding interpolated gravity anomaly values of the four GAS.
Units are in mgal. The first value is the mean difference. The second values is the standard deviation of the differences. The bracketed number corresponds to the number of rejected points where the differences exceeded 50 mgal.

The negative mean values indicate that marine gravity data are lower than GAS grid in this area. The GSFC00, then KMS99 GAS are better matching the marine data than the other grids (Table 12). More points are rejected with the CLS_SHOM99 comparisons than with the other GAS. At this stage, it is difficult to assess if the CLS_SHOM99 is noisier, or if comparison points are rejected because the marine data are noisy. However, Table 13 shows that the KMS99 and GSFC00 GAS are rather similar, and that the KMS99 and the S&S97 GAS are the closest in this area. Maybe because in both determinations, FFT techniques are used with ERS-1 and Geosat GM dataset. Grid differences are always stronger when the CLS_SHOM99 is concerned (~7-8 mgal rms instead of ~5-6 mgal rms for others GAS comparisons). GAS differences in the area, as illustrated by Figure 17 and Figure 18, show that:

- Difference features are characterised by really short scales: less than 50 km wide, but they can exceed 10 mgal.
- The S&S97 and KMS99 GAS exhibit strong trackiness effects.
- Compared to the other GAS, the CLS_SHOM99 present shorter scales, in particular near the strong gradient geoid features.

Differences of grids	Statistics in mgal
CLS_SHOM98.2 – GSFC00	0.12 ± 7.27 (3063)
KMS99 – GSFC00	0.21 ± 5.53 (3217)
S&S97 – GSFC00	0.22 ± 6.00 (3693)
S&S97 – CLS_SHOM98.2	0.11 ± 7.38 (4157)
CLS_SHOM98.2 – KMS99	-0.09 ± 7.11 (3684)
S&S97 – KMS99	-0.02 ± 5.65 (2525)

Table 13: GAS grid difference statistics in the South Japan area. The first value is the mean grid difference. The second values is the standard deviation of the grid differences. Bracketed numbers correspond to reject grid points, where differences exceed 50 mgal.

5.2 The South Atlantic area

Grids	All the data	Removing diff. > 50 mgal
GSFC00	-0.56 ± 5.57	-0.55 ± 5.57 (37)
CLS_SHOM99	-0.04 ± 6.64	-0.03 ± 6.64 (37)
KMS99	-0.68 ± 6.08	-0.69 ± 6.08 (53)
S&S97	-0.28 ± 6.70	-0.21 ± 6.70 (37)

Table 14: Statistics of the differences between the marine gravity measurements in the South Atlantic area and the corresponding interpolated gravity anomaly values of the four GAS.
Units are in mgal. The first value is the mean difference. The second values is the standard deviation of the differences. The bracketed number corresponds to the number of rejected points where the differences exceeded 50 mgal.

79690 marine gravity data were selected in the area 10-20°W/30-40°S. This set of data is fairly more precise than the previous one (about 5-6 mgal). Thus, Table 14 shows that the four GAS are still matching the marine gravity data into their precision level intervals. Note also than compared to the South Japan area, the gravity anomaly spatial variations are not as intense (see Figure 16). However, the analysis of these comparisons (Table 14 and Table 15) reveal similar conclusions than above. Comparisons statistics give the following order of similarities: first the GSFC00, then the KMS99, then the CLS_SHOM99, and finally the S&S97 GAS. The GSFC00 and KMS99 GAS are still really close. The corresponding map of difference (not shown) reveal that GSFC00 gradients are slightly sharper, but the wavelength content of these GAS is comparable. Which is not the case when the CLS_SHOM99 surface is compared to the three others GAS: small scales features of differences are always visible.

Differences of grids	Statistics in mgal
CLS_SHOM98.2 – GSFC00	0.13 ± 4.42 (1208)
KMS99 – GSFC00	0.03 ± 2.42 (1207)
S&S97 – GSFC00	-0.05± 3.67 (1500)
S&S97 – CLS_SHOM98.2	-0.07± 5.17 (1201)
CLS_SHOM98.2 – KMS99	0.09 ± 4.57 (1806)
S&S97 – KMS99	0.02 ± 3.68 (1200)

Table 15: GAS grid difference statistics in the South Atlantic area. The first value is the mean grid difference. The second values is the standard deviation of the grid differences. Bracketed numbers correspond to reject grid points, where differences exceed 50 mgal.

5.3 The North Atlantic area

Between 0-10°W/60-70°N, 32165 marine gravity data were selected. This set of data is the most accurate (less than 5 mgal). It has been validated by EPSHOM (Etablissement Principal du Service Hydrographique et Océanographique de la Marine). We chose this set of data, more accurate, to better infer the accuracy of the different GAS, with respect to the gravity field wavelength contained in the marine data. Three ship legs crossing several interesting features of the gravity field were selected and compared to the four GAS.

This area is also particularly interesting because the GAS can be compared to marine data beyond 66°N. That is, beyond the benefit of the accurate T/P dataset. Thus, the GSFC00 and CLS_SHOM99 that use T/P data to reference the surface, and to reduce altimetric along-track biases would not have this benefit anymore. In the case of the CLS_SHOM99 GAS, it means also that ERS-1 geodetic data are not corrected from the “ocean variability noise”. And because altimetric data density is increasing toward the poles, the effect should be amplified. Thus, a validation in this area can give an upper bound of the GAS inaccuracy.

This is the reason why we decide to proceed to three new determinations of the CLS_SHOM99 GAS in this area, changing the estimation parameters, in order to evaluate their impact in the GAS accuracy compared to the marine data. Also note that this is a way to assess the wavelength description capabilities provided by the ERS-1 geodetic dataset alone, compared to gravity anomaly determinations which are also incorporating the denser Geosat GM dataset. The parameters that are changed –as described in section 2.1.2 – are the section radius of ERS-1 geodetic data, and the upper/lower limits of the covariance model zero-crossing length. These three determinations are parameterised as follow:

- (a) zero-crossing limits: 40-75 km geodetic data selecting radius: ~30 km
- (b) zero-crossing limits: 5-75 km geodetic data selecting radius: ~20 km
- (c) zero-crossing limits: 50-75 km geodetic data selecting radius: ~15 km

By increasing the selection radius, more ERS-1 geodetic data are taken into account in the estimation procedure, and data noise reduction is expected. By changing the limits of the zero-crossing length, smoothing/sharpening of the surface is expected whether the limits are extended/lowered.

Grids	Statistics in mgal (32165)
GSFC00	6.13 ± 4.30 (7.49)
CLS_SHOM99	6.13 ± 5.62 (8.32)
CLS_SHOM99 (a)	*6.14 ± 4.94 (7.88)*
CLS_SHOM99 (b)	*6.11 ± 5.61 (8.29)*
CLS_SHOM99 (c)	*6.13 ± 4.54 (7.62)*
KMS99	6.34 ± 4.63 (7.85)
S&S97	6.33 ± 4.47 (7.75)

Table 16: Statistics of the differences between the marine gravity measurements in the North Atlantic area and the corresponding interpolated gravity anomaly values of the four GAS.
Statistics over 32165 points. Units are in mgal. The first value is the mean difference. The second values is the standard deviation of the differences. The bracketed number corresponds to the RMS (root mean square) value. For description of the three alternative CLS_SHOM99 GAS, see the text.

Like in the two other areas, standard deviations of the marine data/GAS differences (Table 16) are in the accuracy level limits of the marine data. This time, the GAS are all characterised by a lower gravity averaged level. The S&S97 has moved two steps ahead in the order of "similarity" with marine gravity data, and it is close to the KMS99 GAS (Table 17). Which indicates that in this area (partly beyond 66°N), the three surfaces determined using Geosat GM data are closer to the marine gravity data. Note also that grid differences are still larger when the CLS_SHOM99 is concerned, which tend to signify that this surface is noisier.

When we prescribed shorter wavelengths (experiment b) in the CLS_SHOM99 determination, the difference statistics with the marine gravity data are modified (Table 16). Whereas comparisons are improved when the covariance model is "smoother" (experiment a and c). Note that increasing the number of ERS-1 geodetic data in this area has no strong impact on the comparison statistics.

Differences of grids	Statistics in mgal
GSFC00 – CLS_SHOM98.2	0.01 ± 4.64 (4.64)
GSFC00 – KMS99	-0.05 ± 3.09 (3.09)
GSFC00 – S&S97	0.03± 2.92 (2.92)
CLS_SHOM98.2 – S&S97	0.01± 4.32 (4.32)
CLS_SHOM98.2 – KMS99	-0.07 ± 4.54 (4.54)
KMS99 – S&S97	0.09 ± 2.17 (2.18)

Table 17: GAS grid difference statistics in the North Atlantic area. The first value is the mean grid difference. The second values is the standard deviation of the grid differences. Bracketed values are RMS.

The comparisons along the three legs show that in this area:

- The wavelength content of the marine data is about one km, and seems noisy at this scale. Such short scale noise would explain 2-3 mgal in the comparison statistics. The wavelength content of the GAS is about 10-15 km for the CLS_SHOM99 surface, about

15-20 km for both the S&S97 and GSFC00 surfaces, and 20-25 km for the KMS99 surface. Thus all the gravity features of more than 30 km are visible in each surface.

- The sharpest gradients are usually better reproduced by the CLS_SHOM99 GAS. Figure 19 show that the fault between 65.3°N and 66.5°N is well estimated by the CLS_SHOM99 and the GSFC00 GAS.
- Small gravity features are better described by the CLS_SHOM99 GAS (like the two positive anomalies at the northern edge of the fault in Figure 19). However the CLS_SHOM99 GAS exhibits a strong undulation artefact. For instance, 10 km undulations are visible between 63.5°N and 65.2°N in Figure 19. These undulations are witnessing small changes in the marine gravity profile, but they are over-amplified. This might be caused by either the lack of Geosat GM data to constrain the estimation at these short wavelengths, or the noise of the ERS-1 geodetic dataset. Note that these undulations are also visible in the other GAS, in particular, in the GSFC00 surface.

These qualitative results are confirmed once again by the statistics (see Table 18). While rms values indicate that the CLS_SHOM99 GAS is not always presenting less similarities with the marine data (the GSFC00 is always the closest). The higher standard deviations of the differences between the CLS_SHOM99 GAS and the marine data is witnessing the undulation artefact.

The CLS_SHOM99 experiment (c), offers statistics showing better comparison levels with the marine gravity data. In this case, discrepancies are reduced at a level comparable (or better) than the KMS99 or the S&S97 GAS comparisons. Figure 20 reveal that the undulation artefact is reduced, but that the smoothing is not reducing the steep gradients. Moreover, the small features are still better described than in the GSFC00 GAS.

GAS	Leg 1	Leg 2	Leg 3
GSFC00	6.88 ± 2.67 (7.38)	8.31 ± 3.37 (8.97)	7.42 ± 2.69 (7.89)
CLS_SHOM99	7.10 ± 4.49 (8.40)	8.24 ± 4.16 (9.23)	7.63 ± 5.84 (9.61)
CLS_SHOM99 (a)	7.29 ± 3.43 (8.06)	8.21 ± 3.99 (9.13)	7.70 ± 4.19 (8.76)
CLS_SHOM99 (b)	7.14 ± 4.40 (8.39)	8.25 ± 4.15 (9.23)	7.33 ± 5.84 (9.37)
CLS_SHOM99 (c)	7.04 ± 3.03 (7.66)	8.30 ± 3.65 (9.06)	7.72 ± 3.40 (8.43)
KMS99	7.60 ± 3.71 (8.46)	8.84 ± 4.00 (9.70)	6.96 ± 2.21 (7.30)
S&S97	7.49 ± 3.86 (8.43)	8.80 ± 3.77 (9.57)	7.21 ± 2.27 (7.55)

Table 18: Comparisons between GAS and marine gravity data along three ship legs. The first value is the mean grid difference. The second values is the standard deviation of the grid differences. The RMS is in brackets.

6 Discussion and conclusion

Four recent mean sea surfaces and free air gravity anomaly surfaces are validated and compared in this work. The final goal would be to select the surfaces associated with the future Jason-1 or ENVIsat product delivery. The conclusion of this study should help in the selection process. Discussion and conclusions about the MSS and the GAS are given separately, since teams of experts would address separately the selection of these two products. However, although MSS and GAS determined by a given team are close, conclusions concerning MSS may not be appropriate to GAS, and vice-versa. We have demonstrated that the distinct wavelength content of the mean sea height and the gravity anomaly field might be better determined using a given estimation technique in one case, and produce less accurate results in the other case. Note also that only the CLS_SHOM determination schemes provide estimation error field for both the MSS and the GAS. These a-posteriori error fields should be more and more taken into account for operational altimetry (for instance for assimilation procedures).

6.1 The Mean Sea Surfaces

Three 1/16° grid (OSU95, CLS_SHOM98.2, and KMS99), and one 1/30° grid MSS (GSFC00) were compared and validated. In practice, we have performed:

- In a classical way, along track comparisons with precise altimetric mean height profile, to assess the MSS accuracy along satellite ground tracks
- MSS grid to grid comparisons to infer typical wavelengths, DOT content, systematic biases, specific artefacts.

Through these comparisons, we have focused on:

- The MSS accuracy. In fact, we have compared the four MSS to a 3-year T/P and a 2-year ERS-1 mean profiles already included in the CLS_SHOM98.2 MSS determination. However the accuracy of these profiles has been evaluated and it is high. Surprisingly, the 3-year T/P mean profile presents a precision level slightly higher than the 6-year T/P mean profile used by the GSFC team.

  Compared to these profiles, in terms of height differences, the CLS_SHOM98.2 and the GSFC00 MSS offer on the overall comparably good results. The CLS_SHOM98.2 shows better results, but is compared to the same data incorporated in the surface, and the distinct DOT content (3-years instead of 6-years) increases the differences. However, the along-track slope comparisons, which characterises the shortest wavelengths of the MSS are indicating that the CLS_SHOM98.2 MSS is outclassing the three other surfaces.

- The MSS homogeneity. If an MSS is used to reference different types of altimetric data prior any merging procedure, it is necessary to have an oceanwide homogeneity of the DOT content. Note that our 2-year ERS-1 mean profile is consistent with the 3-year T/P mean profile in that sense.

  The KMS99 and the OSU95 MSS contains rather heterogeneous DOT signal: the Tropics and every high oceanic variability area exhibit differences that can exceed 10 cm. In both cases, the geodetic altimetric data low accuracy are contaminating the surfaces. The OSU95 MSS was computed with low accuracy data. And the KMS99 MSS is deduced from the GAS, which explains that wavelength between 100 to 1000 km might be less well estimated.

  The OSU95, CLS_SHOM98.2 and GSFC00 have included a 2-year Geosat ERM mean profile in their determination. Along-track comparisons of the GSFC00 and CLS_SHOM98.2 MSS with the 2-year Geosat mean profile show that these surfaces are not to close to the profile, which is a satisfactory result since we do not expect the MSS to be too close the 1986-1987 DOT content.

Some heterogeneities are also suspected in the GSFC00 MSS, where the DOT content along the T/P and the ERS-1 mean profiles seems slightly different.

- The “trackiness” artefact. Usually caused by merging satellite data which have along-track biases. It is important to remind that this artefact would not appear through along-track comparisons, but need an analysis of the surface.

  These effects appear strongly in the KMS99 and the OSU95 MSS, certainly caused by the data accuracy. Less trackiness is observed in the GSFC00 MSS, which is determined with slopes instead of height of the geodetic data. Then, by using a specific estimation scheme which takes into account the along-track biases, the CLS_SHOM98.2 MSS is free of trackiness effects.
- Short scale resolution. The KMS99 and OSU95 MSS are polluted by noise. But the GSFC00 and CLS8SHOM98.2 surfaces offer the short scale resolution that allow to describe small features of the geoid, as it is already revealed by the along-track slope differences statistics. However, both surfaces still suffer from the “orange-skin” effects.

At this stage, the GSFC00 and CLS_SHOM98.2 MSS offer a good level of accuracy, although we have also observed on the GSFC00 surface an unexplained gap in the North Atlantic area, at 70°N. However, the trackiness effects still contained in the GSFC00 surface tend to nominate the CLS_SHOM98.2 MSS as the good candidate for Jason-1. Note that incorporating Geosat Geodetic Mission data seems to not provide strong benefits in the surface accuracy.

More studies could be carried out to evaluate the different MSS. An independent set of altimetric data could be used to compute then analyse the sea level anomalies (SLA) relative to the four surfaces. In a near future, we propose to use 3-day repeat ERS-1 data to: 1) evaluate SLA noise relative to the four surfaces and 2) crossover discrepancies of short time lag ascending and descending tracks. The second topic allow to corroborate the homogeneity of a given MSS. Then, to fully analyse the spectrum of each MSS, decomposition of the four MSS could be performed in different spectral bands.

6.2 The Free Air Gravity Anomaly Surfaces

Four surfaces have been compared to each other: the Sandwell and Smith’97, the KMS99, the GSFC00, and the CLS_SHOM99 products. In a classical way, the GAS have also been compared to marine gravity data. All the surfaces have a 1/30° (2’) grid resolution. Since all these GAS are determined with altimetric data, all have benefited from a remove/restore procedure where long wavelength of the geoid have been removed to altimetric height, then, after the gravity anomaly determination, the long wavelength gravity contribution of this large scale geoid are added back. Because in the four GAS, EGM96 or an JGM-3 tailored geoid is used, the long wavelength of the surfaces are rather similar. Thus, the comparison only focus on the shortest wavelength of the gravity field.

Qualitatively, the grid comparisons still reveal trackiness effects on the KMS99 and GSFC00 GAS, and also in the S&S97 GAS. Note that these three surfaces have been determined incorporating Geosat geodetic data, noisier than the other altimetric dataset. Because the Earth gravity field is characterised by a more energetic spectrum at short wavelength than the geoid, it is necessary to include in its estimation short scale information. Thus, the gravity anomaly surface determination is a compromise between accuracy, and short scale content.

Three sets of marine gravity data were available. We decided to compare the GAS to these three dataset, although the accuracy and the sampling of the gravity field they provide was not similar. South of Japan, the marine gravity are poorly accurate, with sometimes 10 mgal gaps between different ship-legs. The South Atlantic area is less noisy, but the gravity patterns are there less variable and sharp. Finally, the North Atlantic area offer a more accurate set of marine gravity data (better than 5 mgal). In any case, the discrepancies between the marine data and the GAS span in the in-situ data accuracy. However, a general result appears over the three set of comparisons. Relative to the marine data, the GSFC00 GAS is the closest surface. Then the KMS99 and the S&S97 occupy the next rank. On the overall, the CLS_SHOM99 GAS seems to have deficiency in fitting the marine gravity anomaly signal. But looking more carefully, profile after profile, because marine data provide irregular sampling of the gravity field, alternatively, one GAS can better match these in-situ data than the others.

In practice, the GSFC00, the KMS99 and the S&S97 GAS were determined with spatial filtered altimetric data (with cut-off of 12 km or higher), maybe to reduce the noise of ERS-1 or Geosat geodetic data. Whereas the CLS_SHOM99 GAS, not incorporating the dense Geosat GM dataset, had no filtering procedure. Moreover, by using locally variable covariance models, the impact of the ERS-1 geodetic noise could be stronger near sharp geoid gradient areas. In fact, grid comparisons show that alternatively the GSFC00, the KMS99 and the S&S97 are close to each other. While the CLS_SHOM99 still present really short scales differences, usually located in highly variable areas.

A careful analysis of the four GAS along three marine gravity ship-legs in the North Atlantic shows first that the typical resolution of these surfaces are: 10-15 km, 15-20 km and 20-25 km for respectively the CLS_SHOM99, the GSFC00 and the S&S97, and the KMS99 GAS. Second, the shorter wavelength content allows the CLS_SHOM99 to better match some gravity anomaly perturbations, however, it often corrupts the surface with a short scale undulation artefact. Thus, we have proceeded to some sensitivity study in order to check whether more ERS-1 geodetic data, or a smoothing effect applied through more extended correlation functions would improve the comparisons. By prescribing longer correlation length, the CLS_SHOM surface is better matching the marine gravity data signal, with a level comparable to the other surfaces, and small gravity features are still properly described. Note that these last comparisons are carried out beyond 66°N, which exclude the benefit of precise T/P data. In that sense, the level of discrepancies is probably an upper bound of the inaccuracy of the CLS_SHOM99 GAS. Note also that such variable covariance model used in the CLS_SHOM99 GAS determination was not used for the CLS_SHOM98.2 MSS. That is, artefacts due to too short covariance functions will not appear in the MSS.

At this stage of our comparisons, the GSFC00 free air gravity anomaly surface offers an overall description of the Earth gravity field that best matches marine gravity data. However, we have clearly demonstrated that a gravity surface incorporating only ERS-1 geodetic data, offers a description of the gravity field of the same precision order than those incorporating both ERS-1 and Geosat GM dataset. Thus, away from high latitudes, it not yet sure that Geosat geodetic data provide more information than noise. The CLS_SHOM99 might need to use smoother correlation function to avoid some small scales artefacts. In any case, these surfaces should be compared to other set of marine gravity data, and maybe in configurations closer to the coast where stronger gradients are expected.

7 Captions

7.1 Figure Captions

7.2 Table Captions

8 Reference

Andersen, O. B., and P. Knudsen, 1998 : Global marine gravity field from the ERS-1 and Geosat geodetic mission altimetry. *J. Geophys. Res.* Vol. 103, C4, 8129-8137.

Andersen, O. B, P.L. Woodworth, and R.A. Flather, 1995 : Intercomparison of recent global ocean tide models. . *J. Geophys. Res*. 100, C12 , 25261-25282.

Archiving, Validation, and Interpretation of Satellite Oceanographic Data, AVISO Handbook for merged TOPEX/POSEIDON products, 3rd ed., *Handb, AVI-NT-02-101-CN*, Toulouse, France, 1996.

Cartwright, D.E., and R.D. Ray, 1990 : Oceanic tides from Geosat altimetry. . *J. Geophys. Res*., 95, 3069-3090.

Centre ERS d'Archivage et de Traitement, 1994 : ERS-1 Altimeter Products User manual, *Handb, C1-EX-MUT-A21-01-CN*, Brest, France.

Centre ERS d'Archivage et de Traitement, 1996 : Altimeter and Microwave Radiometer ERS Products User manual, *Handb. C2-MUT-A-01-IF*, Brest, France.

Cheney, R.E., J.G. Marsh, and B.D. Beckley, 1983: Global mesoscale variability from collinear tracks of Seasat altimeter data. *J. Geophys. Res*., 88, 4343.

Eanes, R.J., and S.V. Bettadpur, 1995: The CSR3.0 Global Ocean Tide Model. *Rep.* CSR-TM-95-06, Cent. For Space Res., Univ. Of Texas, Austin.

Forsberg, R., 1987 : A New covariance model for inertial Gravimetry and Gradiometry. *J. Geophys. Res*., 92, 1305-1310.

Hernandez, F., 2000 : Improving mean sea level calculation from satellite altimetry. Submitted to *Journ. of Atmos. and Oceanic Technol.*

Jordan, S.K, 1972 : Self consistent statistical models for the Gravity Anomaly, Vertical Deflections and Undulations of the Geoid. *J. Geophys. Res*., 77, 3360-3370.

Knudsen, P., and O. B. Andersen, 1998 : Global marine gravity and mean sea surface from multimission satellite altimetry. In "Geodesy on the Move, Gravity, geoid, geodynamics and Antarctica", Proceedings IAG scientific assembly, Rio de janeiro, sept 3-9 1997, Eds, Forsberg, Feissel and Dietrich. IAG symposia, 119, 132-138, Springer, Berlin, 1998.

Knudsen, P., and O. B. Andersen, 1997 : Improved recovery of the Global Marine Gravity Field from the GEOSAT and ERS-1 Geodetic Mission Altimetry. In "Gravity, Geoid, and Marine Geodesy", Proceedings IAG scientific assembly, Tokyo, sept 3-oct 5 1996, Eds, Segawa, Fujimoto, and Okubo. IAG symposia, 117, 429-436, Springer, Berlin, 1997.

Koblinsky, C.J., R. Ray, B.D. Beckley, Y.-M. Wang, L. Tsaoussi, A. Brenner, and R. Williamson, 1998 : NASA Ocean Altimeter Project, Report 1: Data Processing Handbook. *NASA technical Memorandum, NASA/NT-1998-208605*.

Le Traon, P.-Y., and F. Ogor, 1998 : ERS-1/2 orbit improvement using TOPEX/POSEIDON: the 2 cm challenge. *J. Geophys. Res.*, 103, 8045-8057.

Le Traon, P.-Y., F. Nadal, and N. Ducet, 1998 : An improved mapping method of multisatellite Altimeter data. *J. Atm. Oc. Tech.*, **15**, 522-534.

Lemoine F. G., D. E. Smith, L. Kunz, R. Smith, E. C. Pavlis, S. M. Klosko, D. S. Chinn, M. H. Torrence, R. G. Williamson, C. M. Cox, K. E. Rachlin, Y. M. Wang, S. C. Kenyon, R. Salman, R. Trimmer, R. H. Rapp, et R. S. Nerem, 1996 : The development of the NASA GSFC and NIMA Joint Geopotential Model. Proceeding paper for the International Symposium on Gravity, Geoid, and Marine Geodesy (GRAGEOMAR, 1996). The university of Tokyo, Tokyo, Japan.

Levitus, S., 1982 : Climatological atlas of the world ocean Prof. Pap. 13, 173pp., Natl. Ocean and Atmos. Admin., Silver Spring, Md.

Levitus, S., R. Burgett and T.P. Boyer, 1994a : World ocean atlas 1994 volume 3 : Salinity. NOAA Atlas NESDIS 3. 99pp.

Levitus, S., and T.P. Boyer, 1994b : World ocean atlas 1994 volume 4 : Temperature. NOAA Atlas NESDIS 4. 117pp.

Meier, S., 1981 : Planar Geodetic Covariance Functions. *Rev. Geophys. Space Phys.*, 19, 673-686.

Nerem, R.S., et al., 1994 : Gravity model development for TOPEX/POSEIDON : Joint Gravity Models 1 and 2. *J. Geophys. Res.,* 99, 24421-24447.

Rapp, R.H. and N.K. Pavlis, 1990 : The development and analysis of geopotential coefficient models to spherical harmonic degree 360. *J. Geophys. Res.,* 95, (B13) 21885-21911.

Rapp, R.H., Y.M. Wang, and N.K. Pavlis, 1991 : The Ohio State 1991 geopotential and sea surface topography harmonic coefficient models. Rep. 410, Dept. Geod. Sci. Surv., The Ohio State Univ., Colombus, USA.

Rapp, R.H, 1998 : Past and Future Developments in Geopotential Modelling. In "Geodesy on the Move, Gravity, geoid, geodynamics and Antarctica", Proceedings IAG scientific assembly, Rio de janeiro, sept 3-9 1997, Eds, Forsberg, Feissel and Dietrich. IAG symposia, 119, 58-78, Springer, Berlin, 1998.

Shum et al., 1997 : Accuracy assessment of recent ocean tidal models. *J. Geophys. Res.,* 102, 25173-25194.

Sandwell, D.T., and W.H.F. Smith, 1997 : Marine gravity anomaly from Geosat and ERS-1 altimetry. . *J. Geophys. Res.,* 102, 10039-10054.

Tapley, B., M. Watkins, J.C. Ries, G. Davis, R. Eanes, S. Poole, H. Rim, B. Schutz, C.K. Shum, R.S. Nerem, F. Lerch, J.A. Marshall, S. Klosko, N. Pavlis, and R. Williamson, 1996 : The Joint Gravity Model 3. *J. Geophys. Res.,* 101, 28029-28049.

Tscherning, C.C., R. Forsberg, and P. Knudsen, 1992 : The GRAVSOFT package for geoid determination. Proc. First workshop on European Geoid, Prague, May, 1992.

Tarantola, A., and B. Valette, 1982: Generalized nonlinear inverse problems solved using the least square criterion. *Rev. Geophys*., 20, 219-233.

Wang, Y-M, 2000 : The satellite altimeter data derived Mean Sea Surface GSFC98. *Geophys. Res. Letters*, 27, 5, 701-704.

Yi, Y., 1995 : Determination of gridded mean sea surface from TOPEX, ERS-1, and Geosat altimeter data. Rep. 434, Dept. Geod. Sci. Surv., The Ohio State Univ., Colombus, USA.

9 Figures

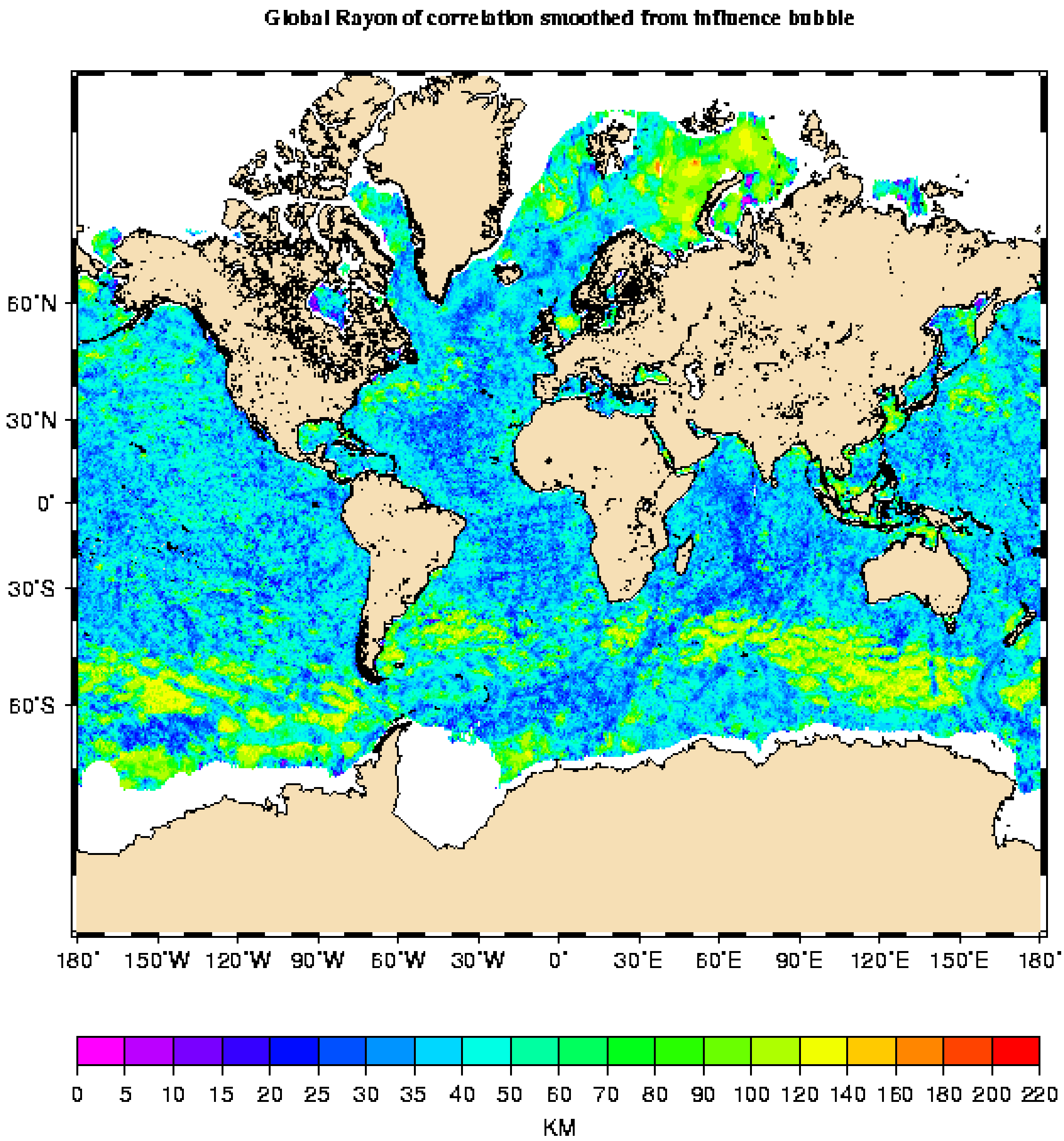

Figure 1: Global map of the zero-crossing (in km) of the gravity anomaly covariance models in each suboptimal box.

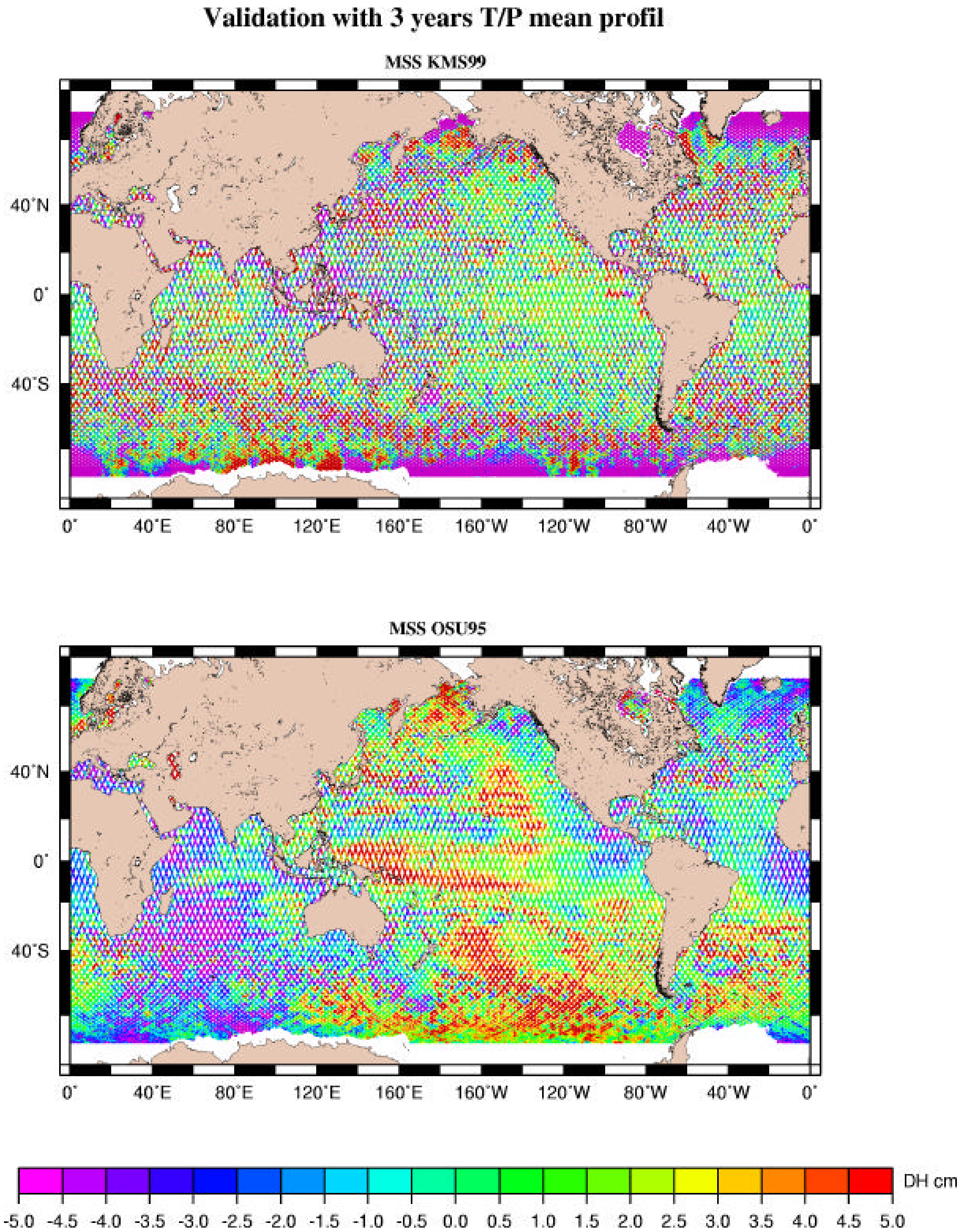

Figure 2: Global map of the along-track height differences between the 3-year T/P mean profile and KMS99 (top) and OSU95 (bottom) MSS.

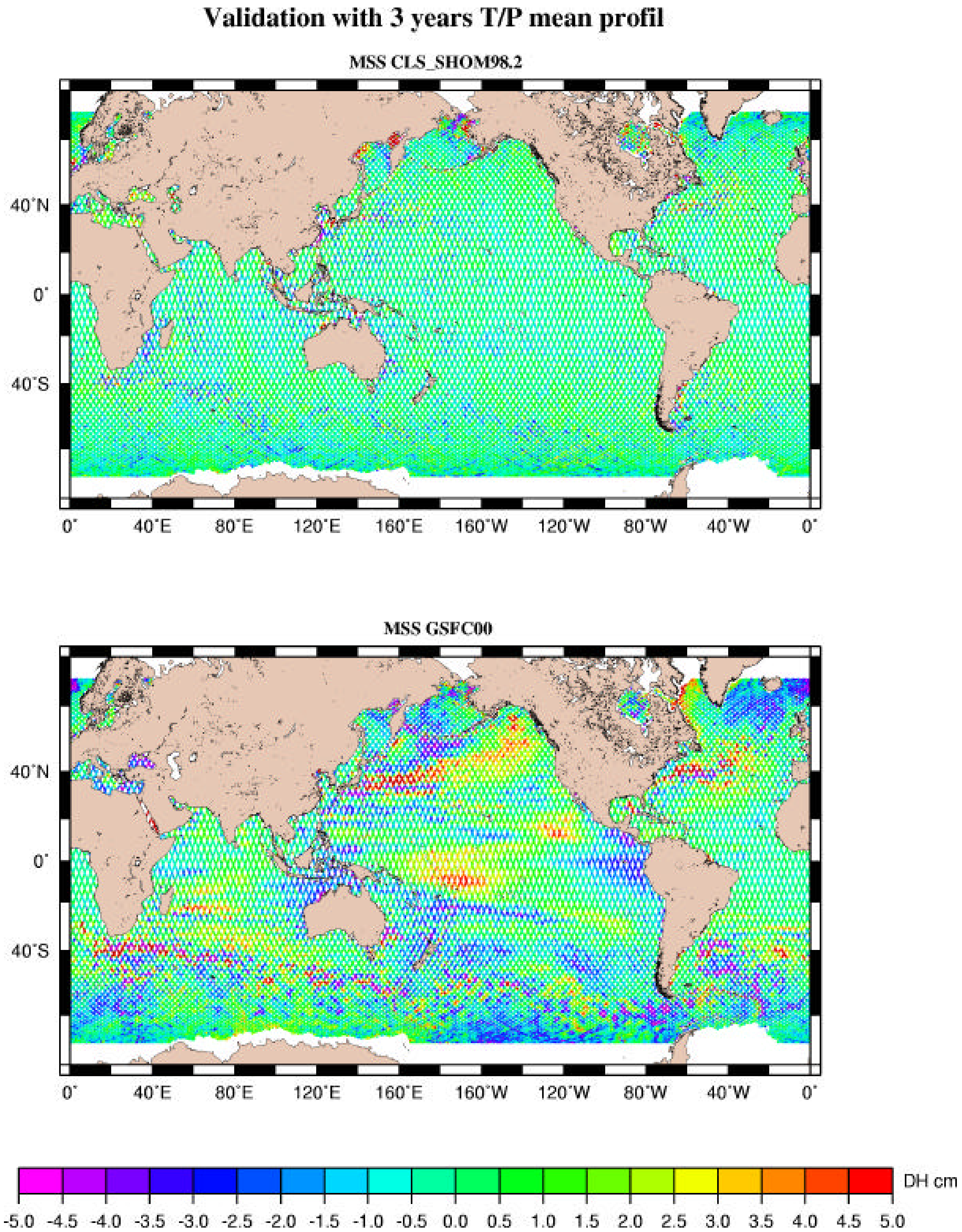

Figure 3: Global map of the along-track height differences between the 3-year T/P mean profile and CLS_SHOM98.2 (top) and GSFC00 (bottom) MSS.

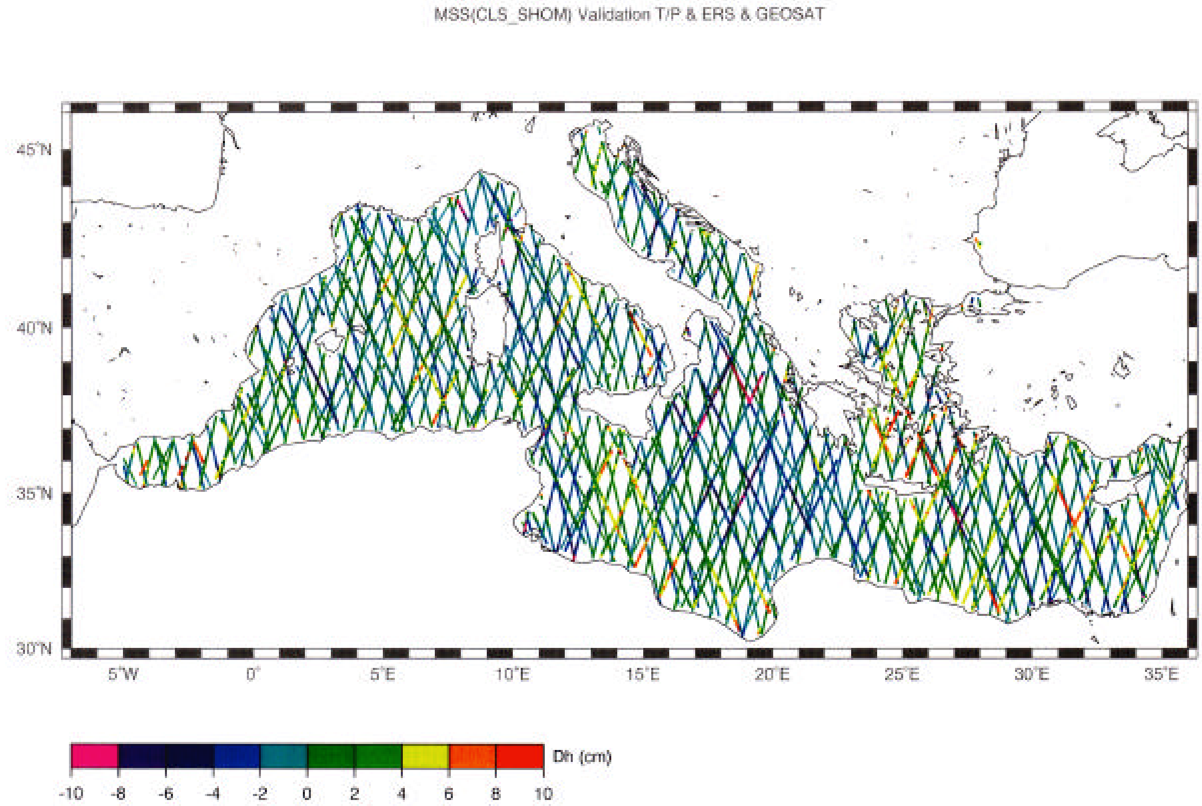

Figure 4: Along-track height differences (cm) between the CLS_SHOM98.2 MSS and the 3-year T/P, 2-year ERS-1 and 2-year Geosat mean profiles in the Mediterranean Sea. T/P tracks are the most inclined, ERS-1 tracks the least. Geosat tracks are thicker.

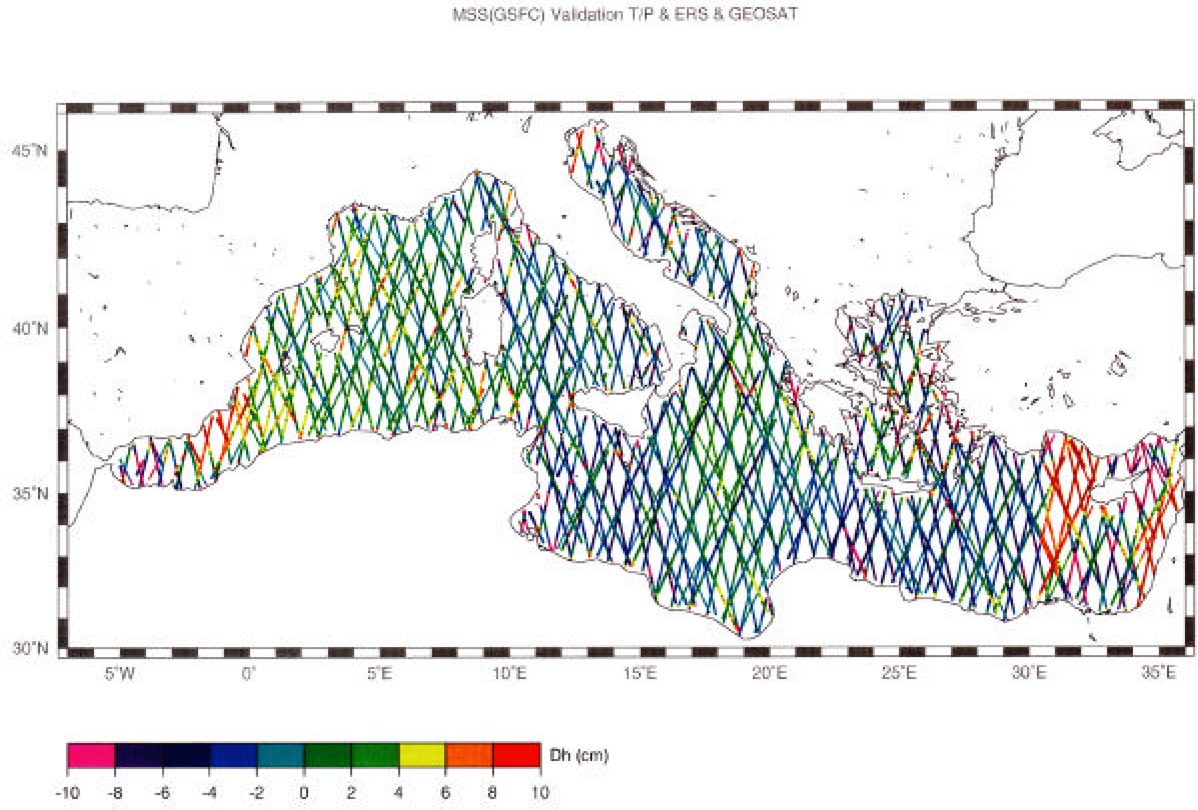

Figure 5: Along-track height differences (cm) between the GFSC00 MSS and the 3-year T/P, 2-year ERS-1 and 2-year Geosat mean profiles in the Mediterranean Sea. T/P tracks are the most inclined, ERS-1 tracks the least. Geosat tracks are thicker.

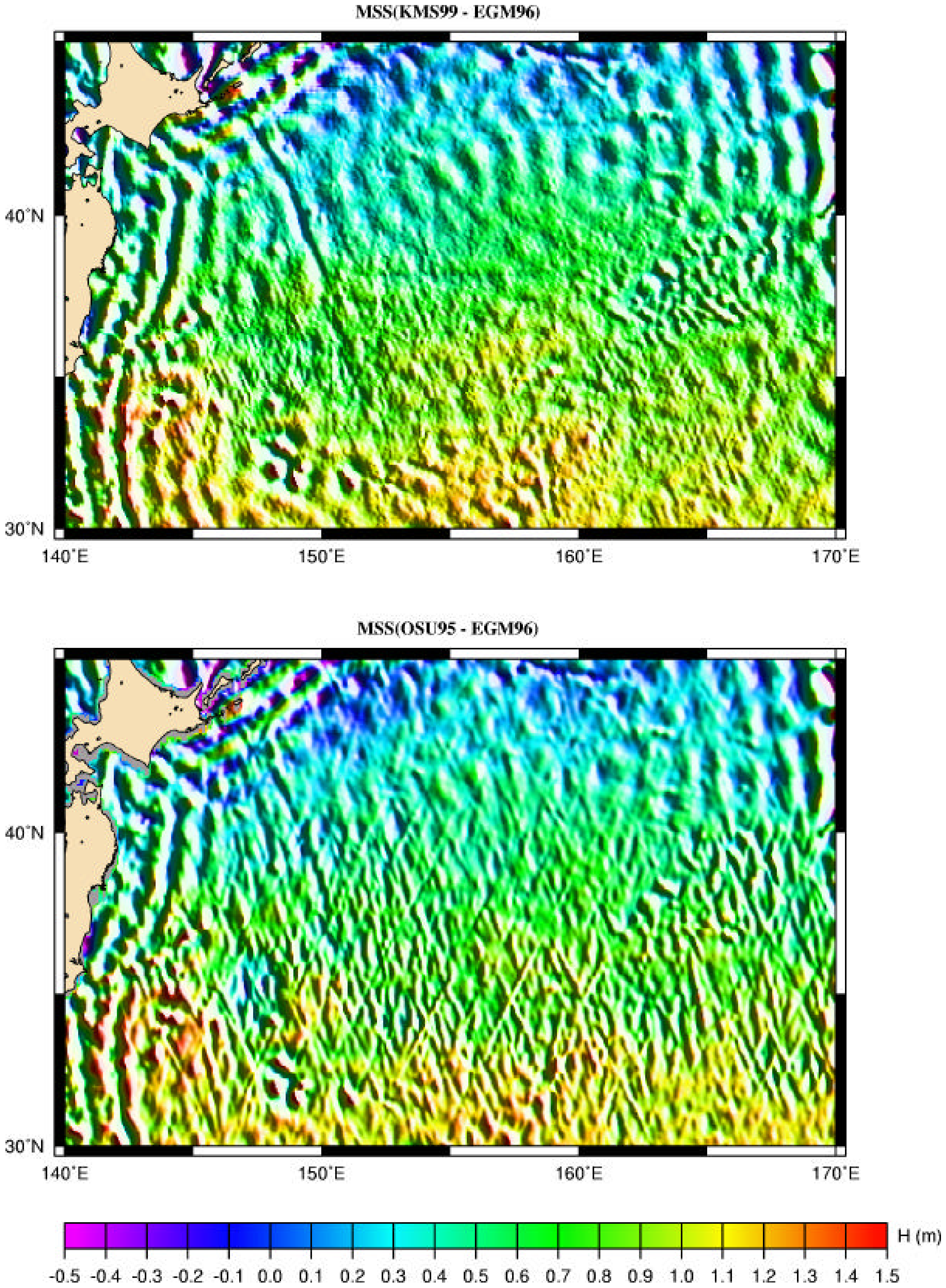

Figure 6: Zoom of the KMS99 (top) and OSU95 (bottom) MSS relative to EGM96 in the Pacific ocean, east of Japan. Heights are meters.

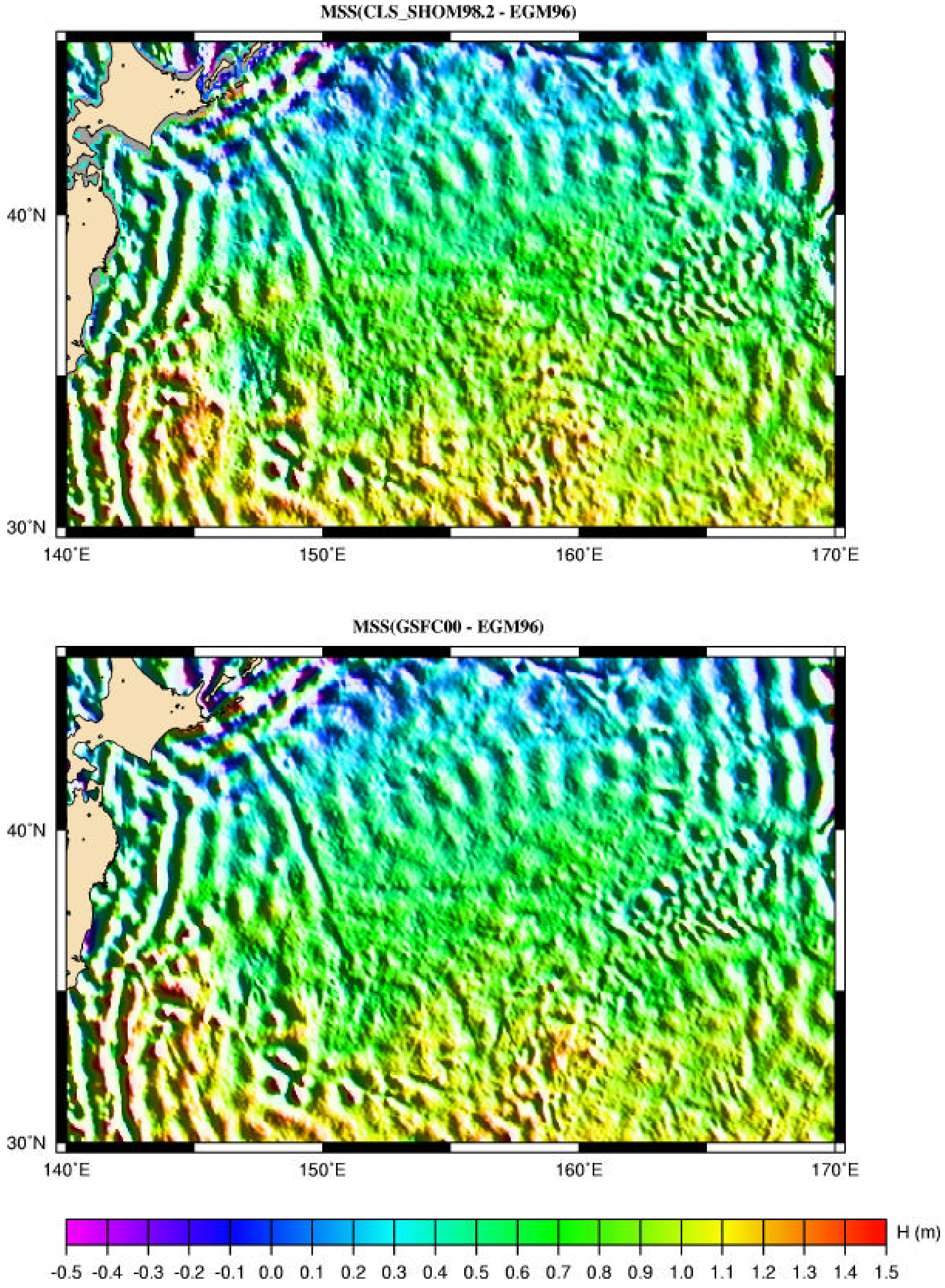

Figure 7: Zoom of the CLS_SHOM98.2 (top) and GSFC00 (bottom) MSS relative to EGM96 in the Pacific ocean, east of Japan. Heights are meters.

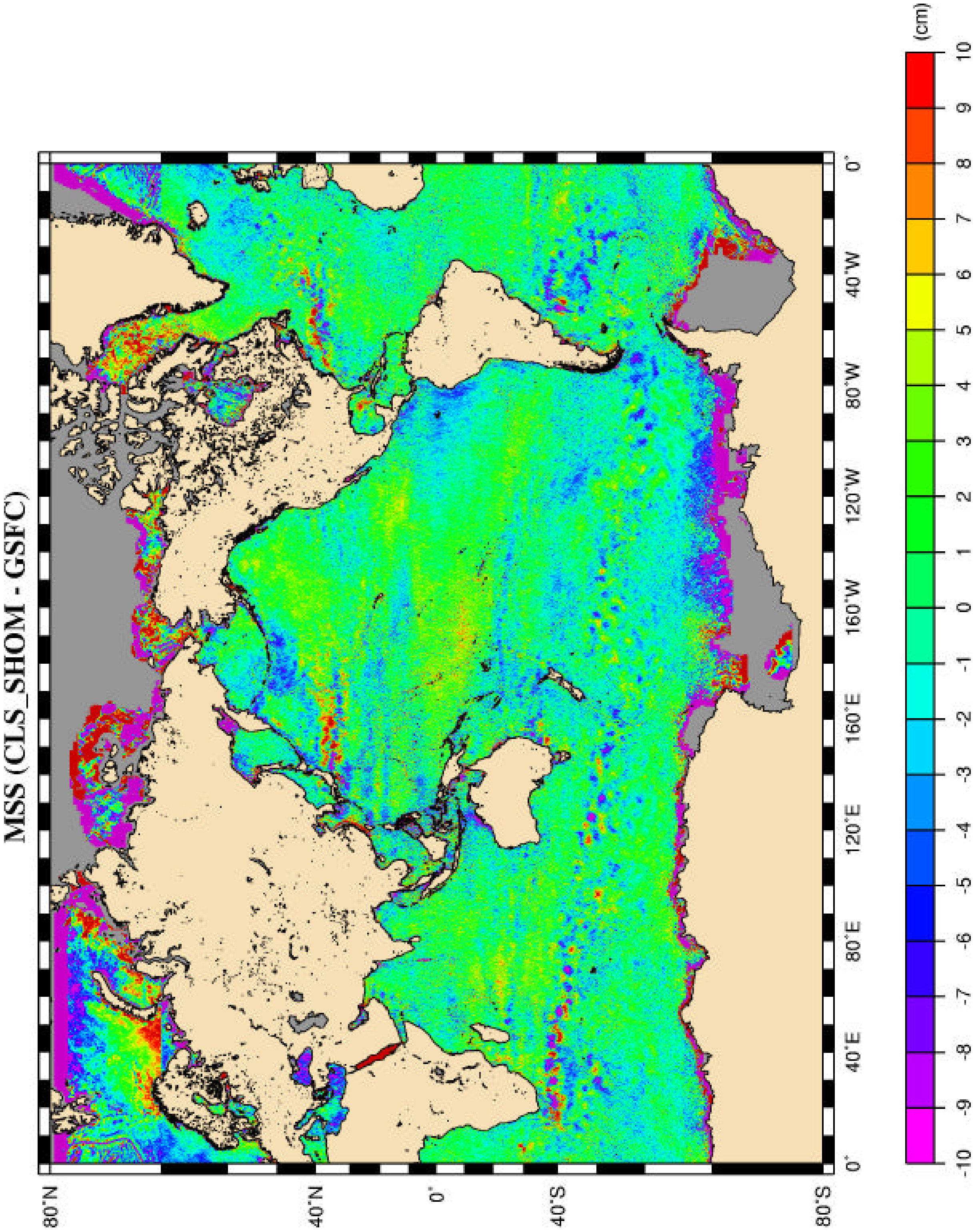

Figure 8: Global height differences (in cm) between the CLS_SHOM98.2 and the GSFC00 MSS.

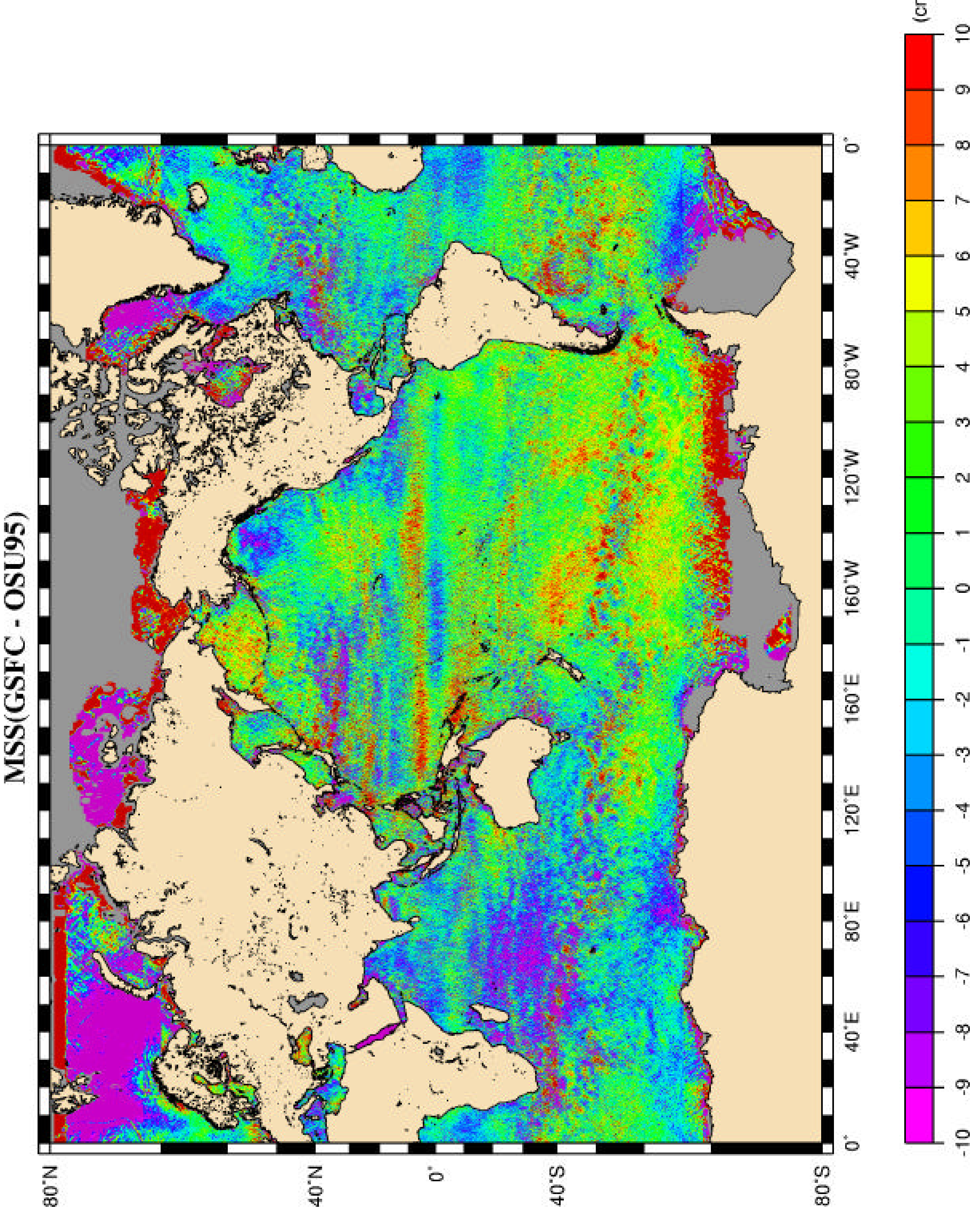

Figure 9: Global height differences (in cm) between the GSFC00 and the OSU95 MSS.

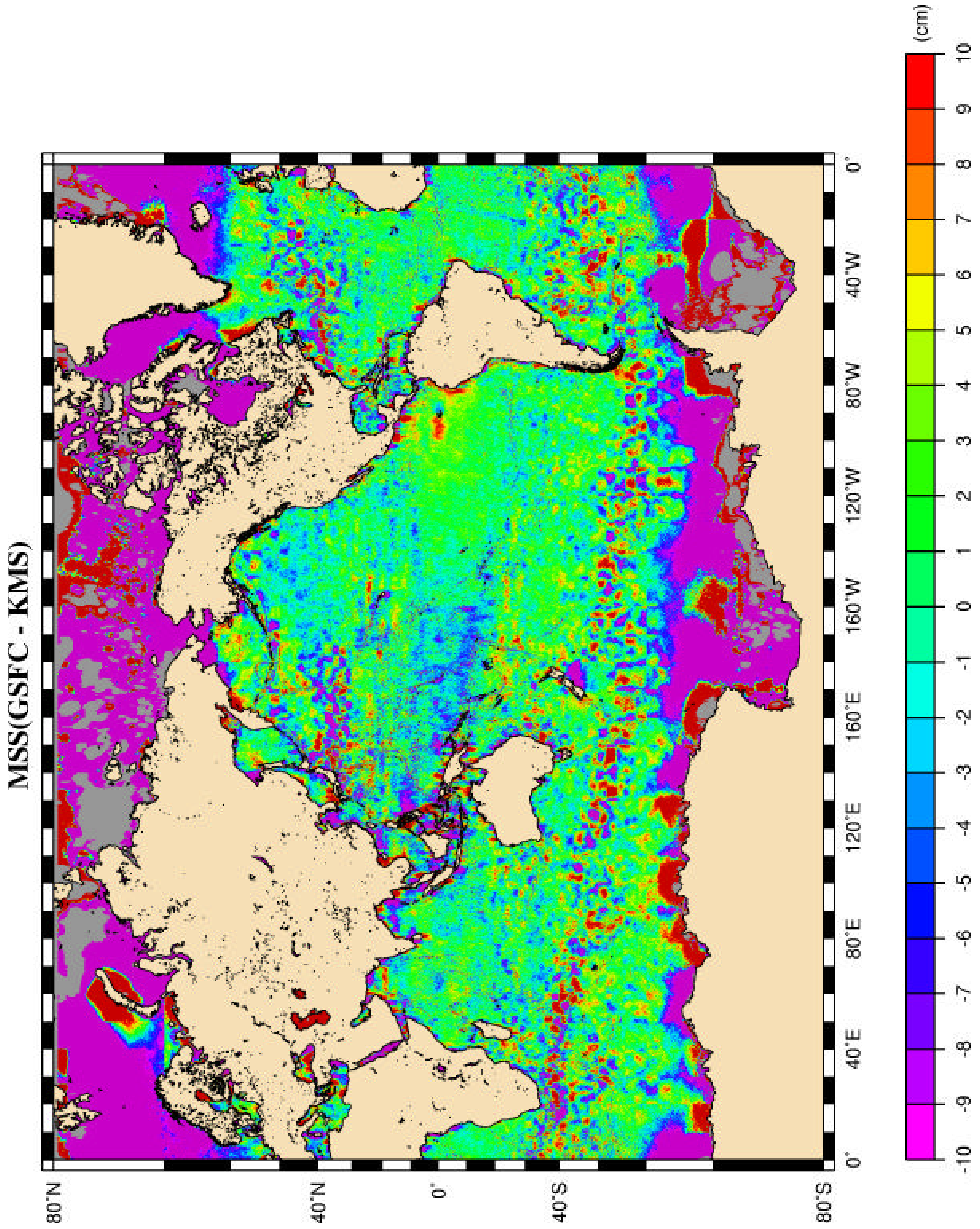

Figure 10: Global height differences (in cm) between the KMS99 and the GSFC00 MSS.

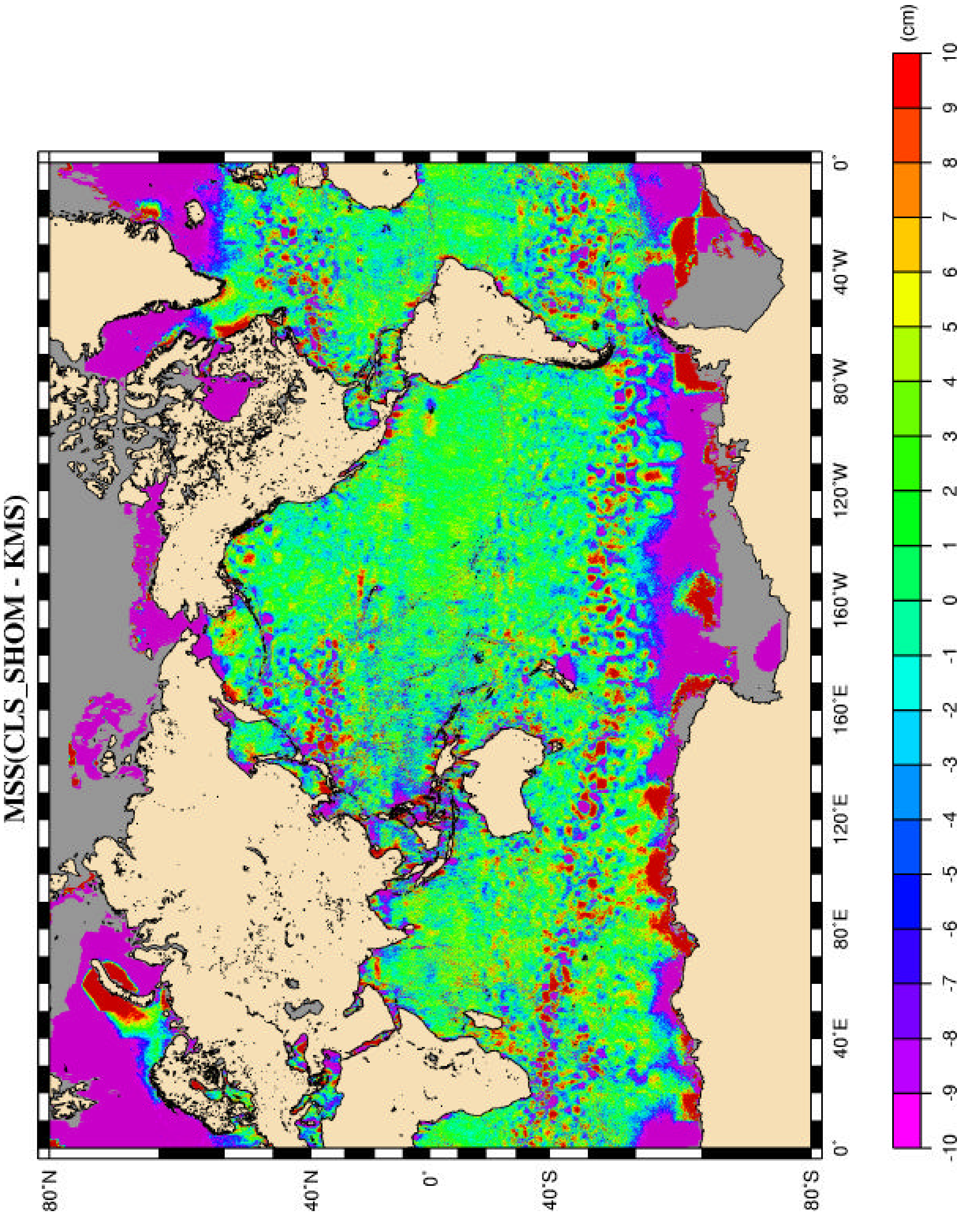

Figure 11: Global height differences (in cm) between the CLS_SHOM98.2 and the KMS99 MSS.

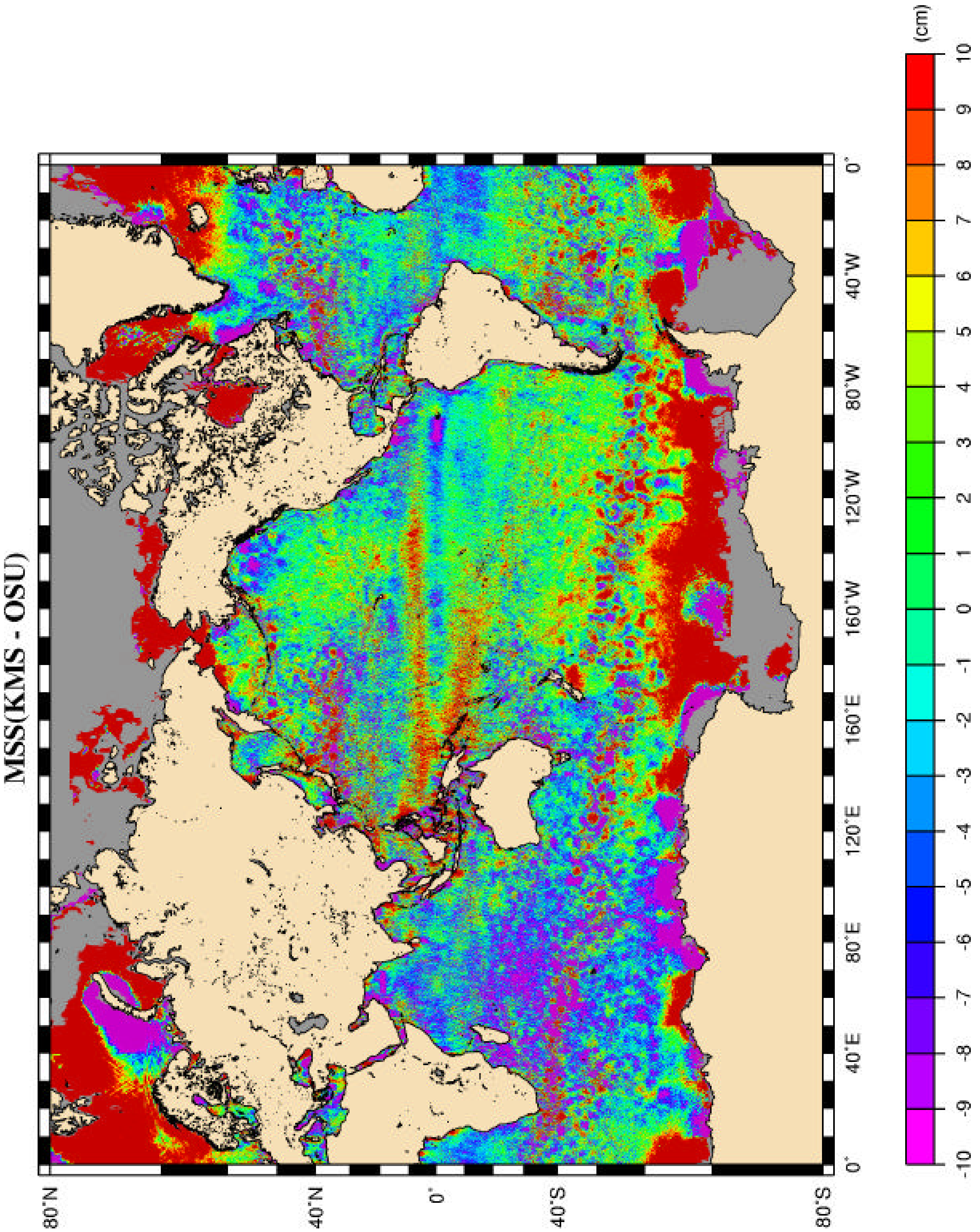

Figure 12: Global height differences (in cm) between the KMS99 and the OSU95 MSS.

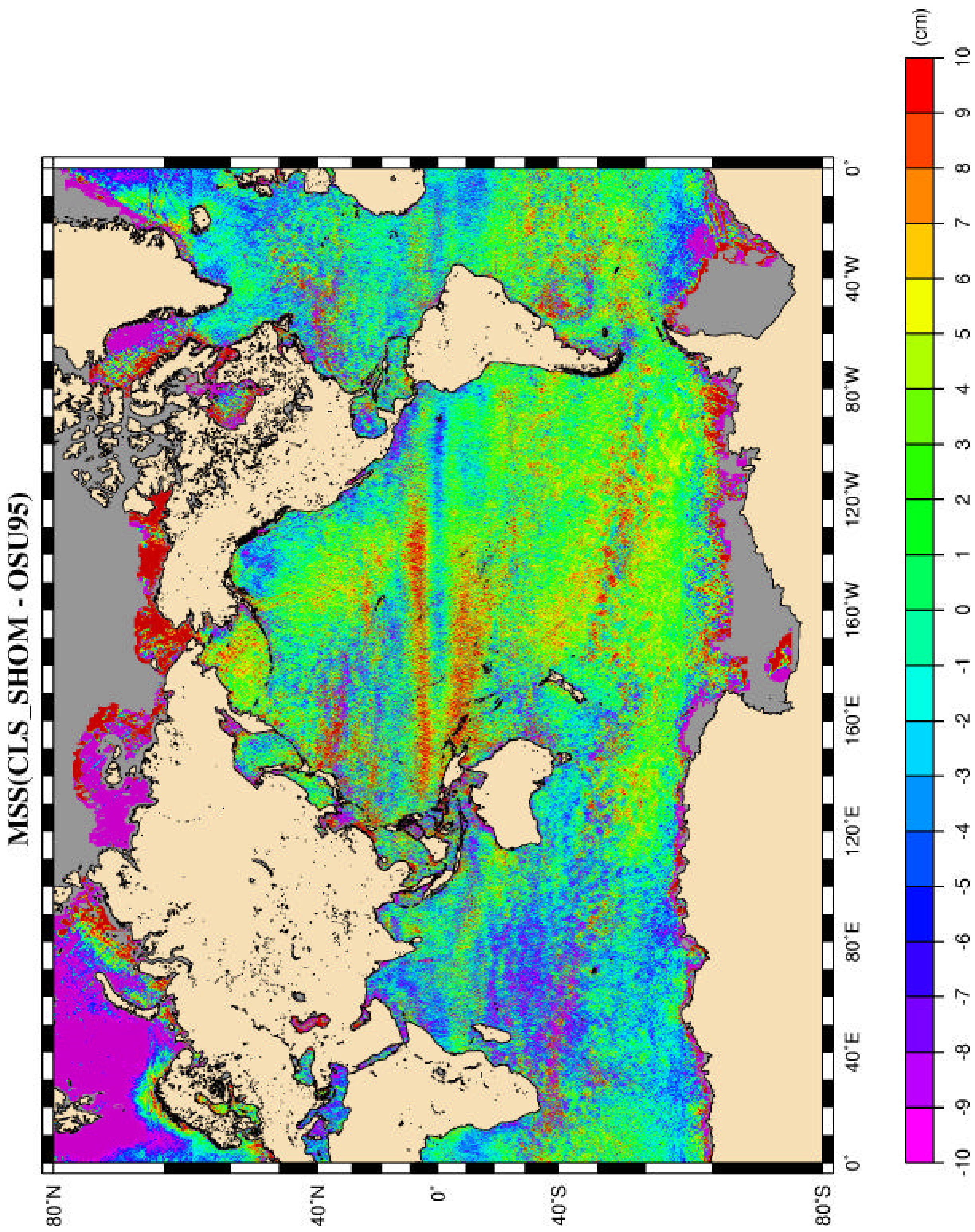

Figure 13: Global height differences (in cm) between the CLS_SHOM98.2 and the OSU95 MSS.

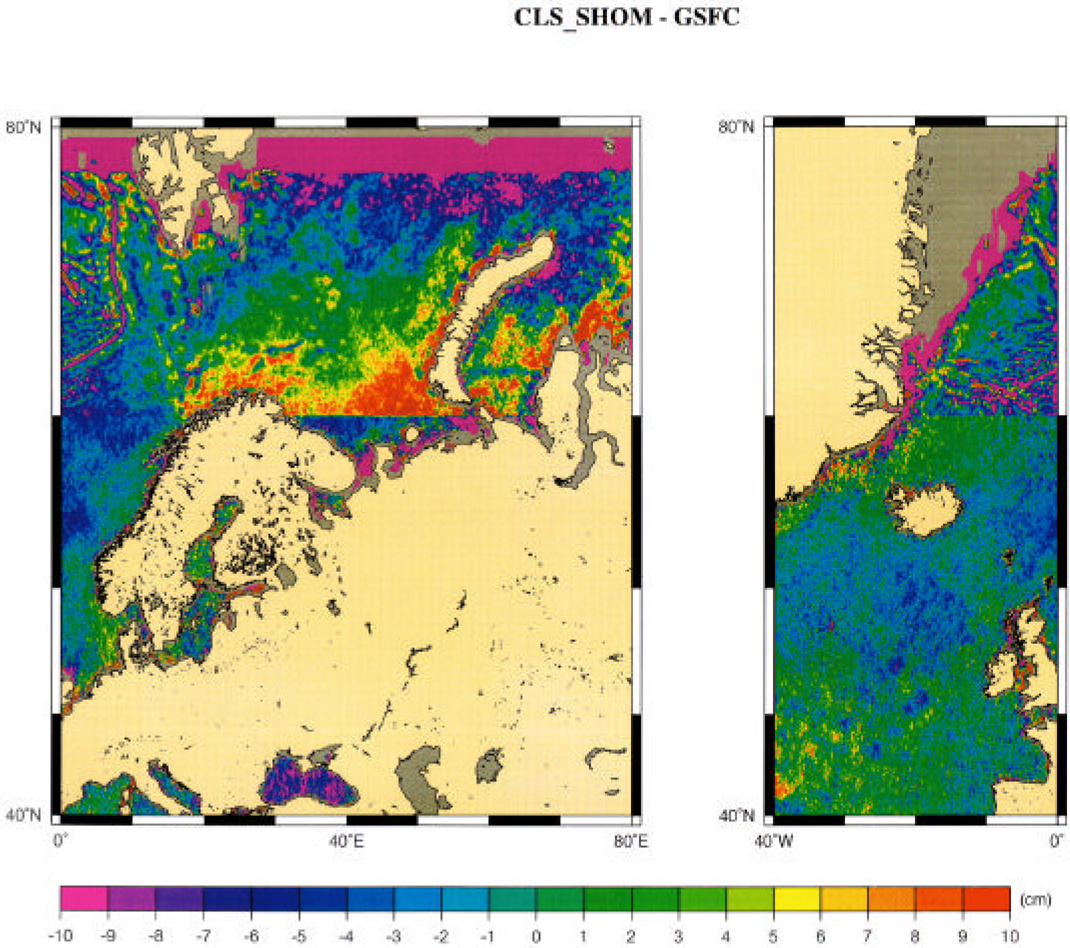

Figure 14: Zoom in the Arctic area of the grid differences between the GSFC00 and CLS_SHOM98.2 MSS (in cm).

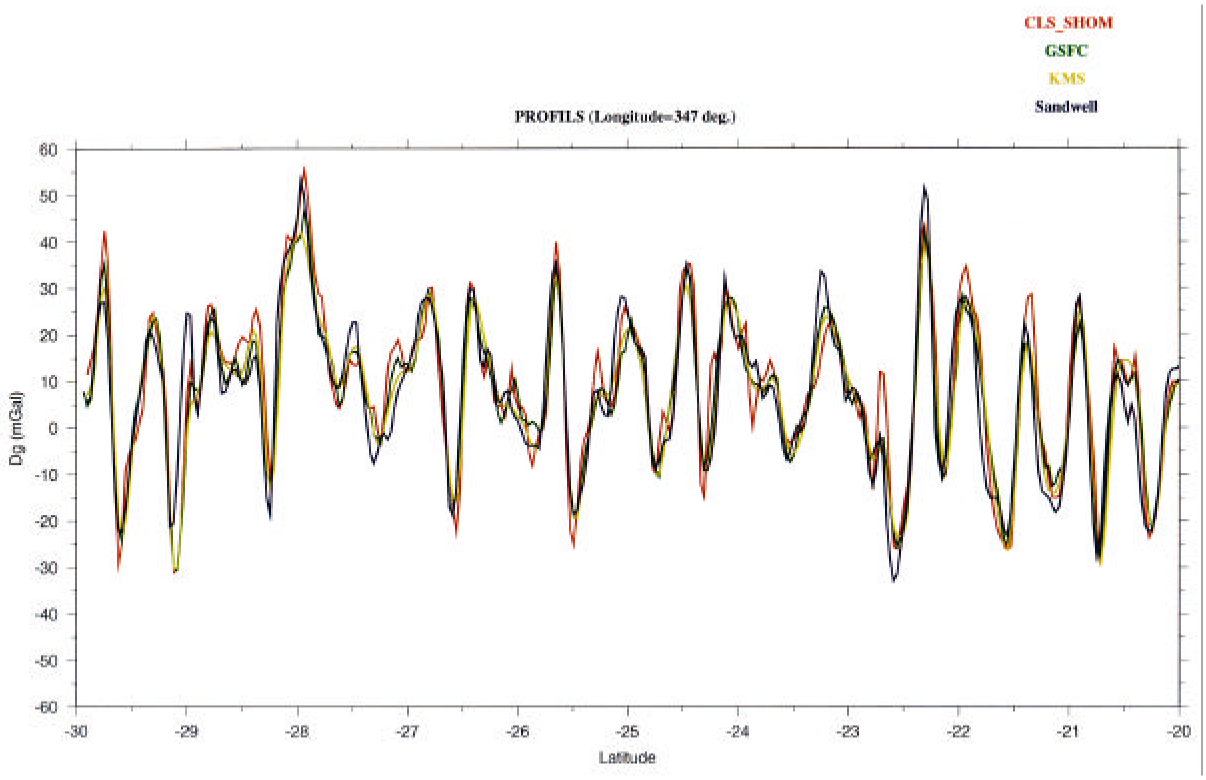

Figure 15: The profiles of the four surfaces (in mgal) along 347°E, between 20-30°S.

Validations of gravity anomaly with gravi-marines data

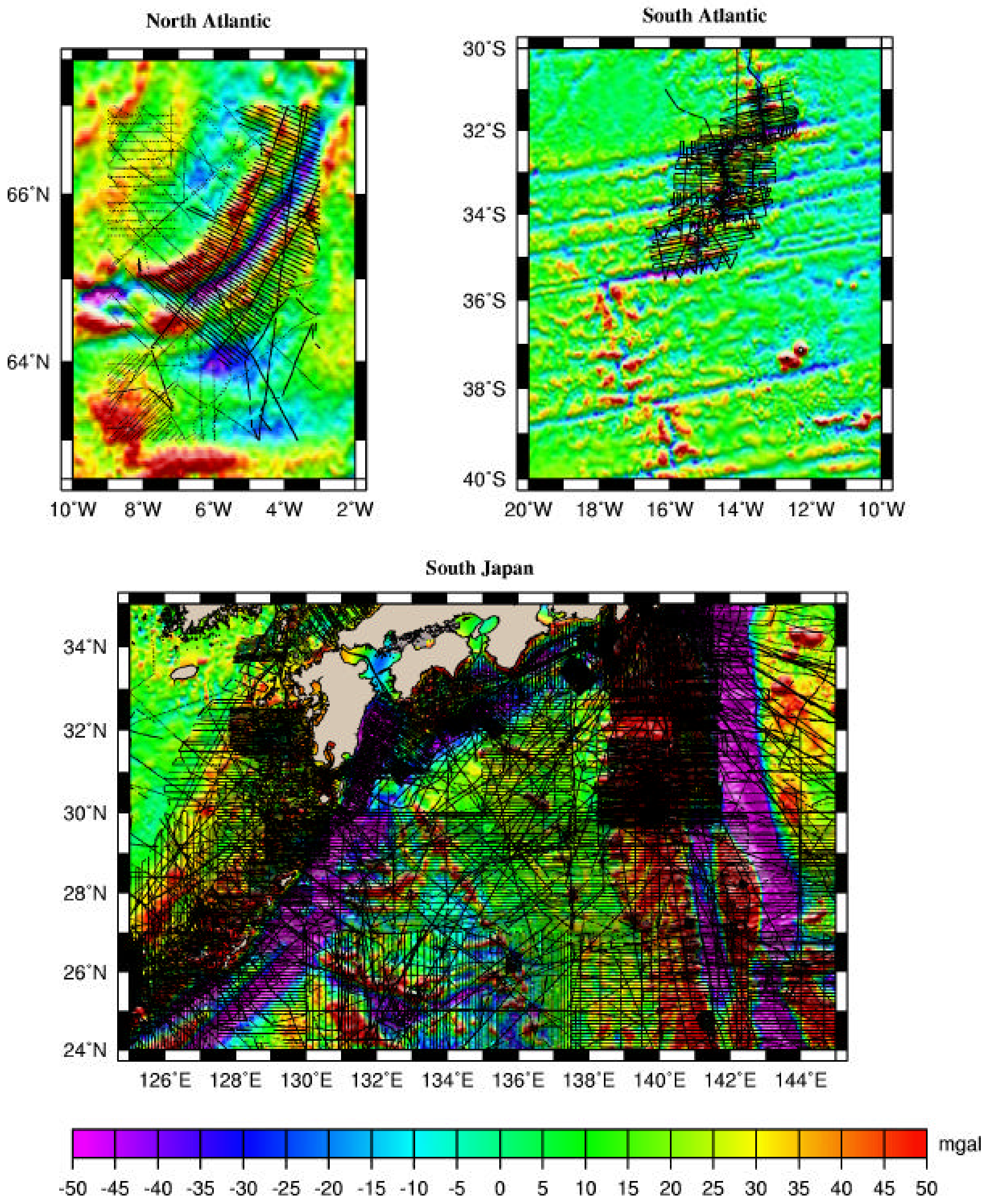

Figure 16 Three marine gravity dataset for comparing with GAS. Legs of ship measurements are plotted in black, above the CLS_SHOM99 GAS.

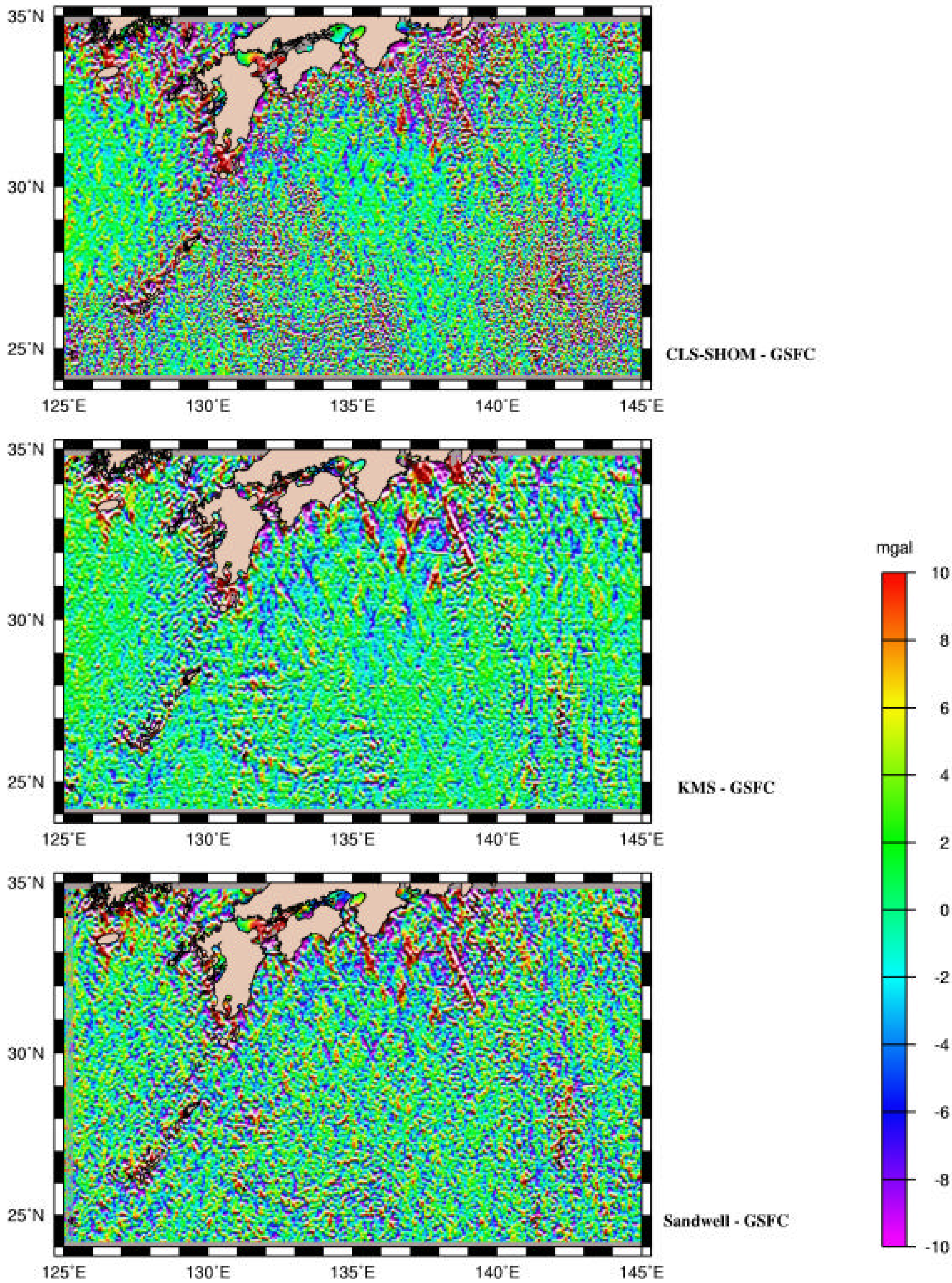

Figure 17: Differences between free air gravity anomaly surfaces in the South Japan area/

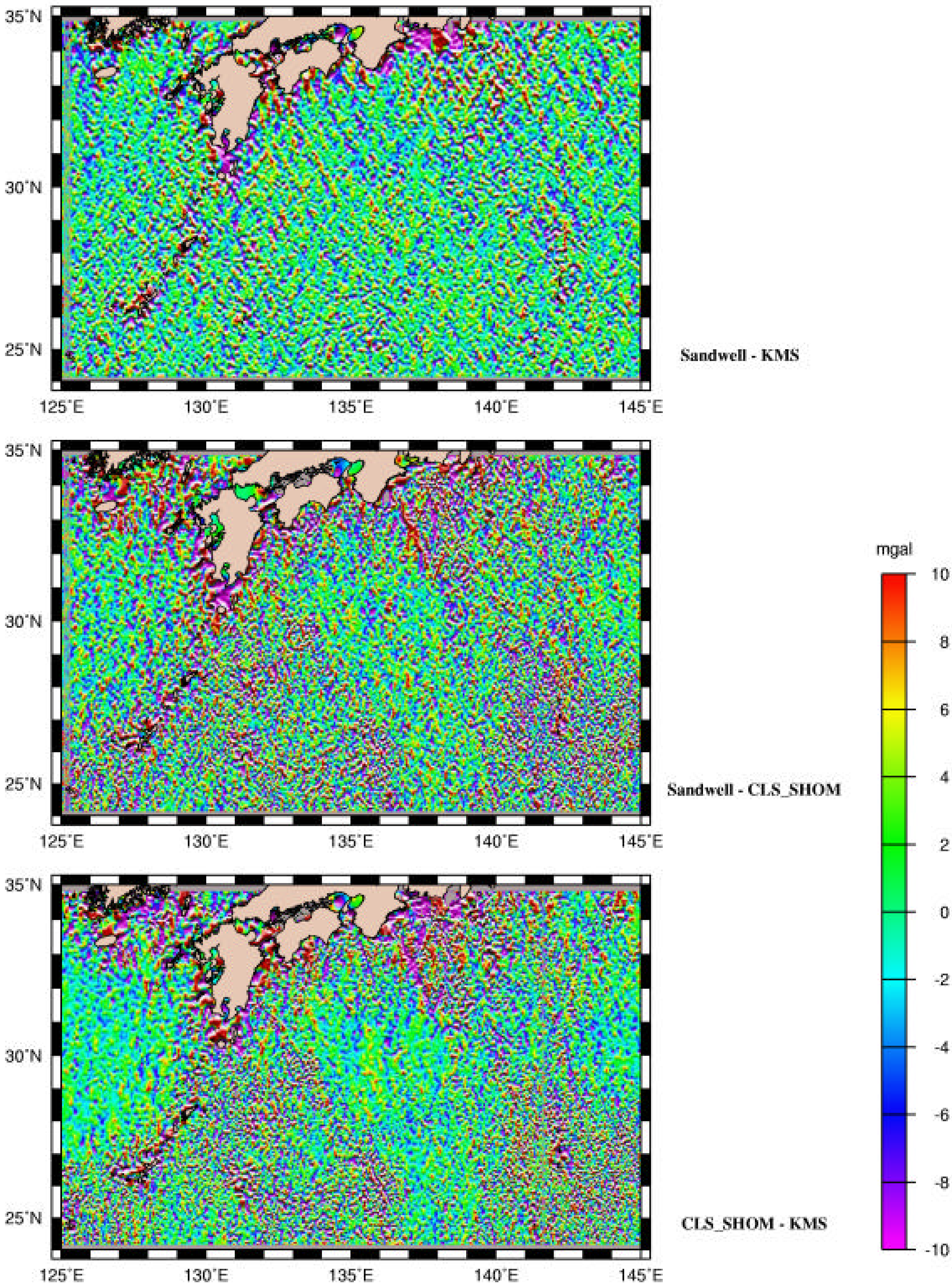

Figure 18: Differences between free air gravity anomaly surfaces in the South Japan area (cont'd).

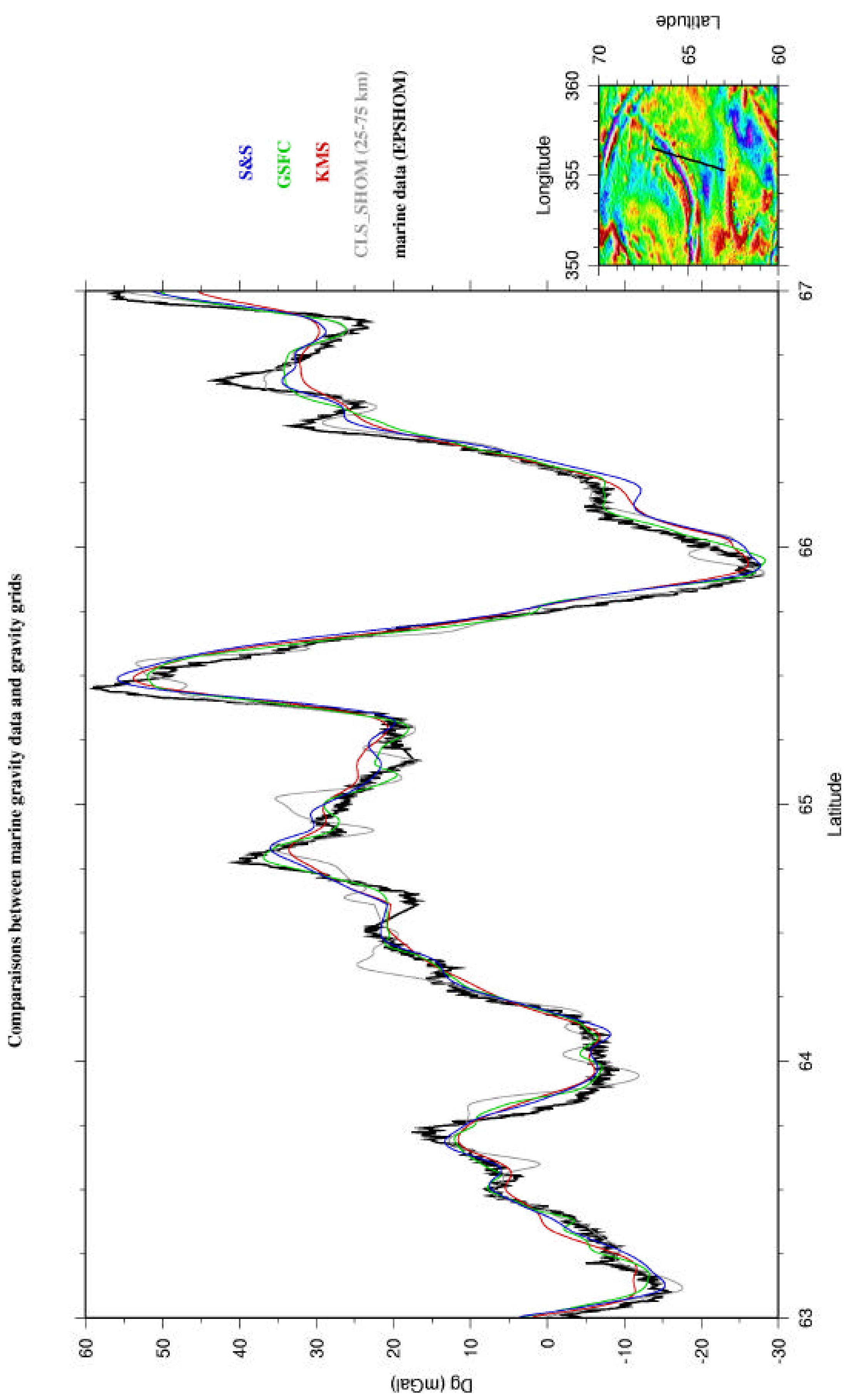

Figure 19: Comparisons between the marine gravity data (black) and the GSFC00 (green), the S&S97 (blue), the KMS99 (red), and the CLS_SHOM99 (grey) GAS along leg 2 (in mgal). The position of the leg is represented in black on the right lower side map.

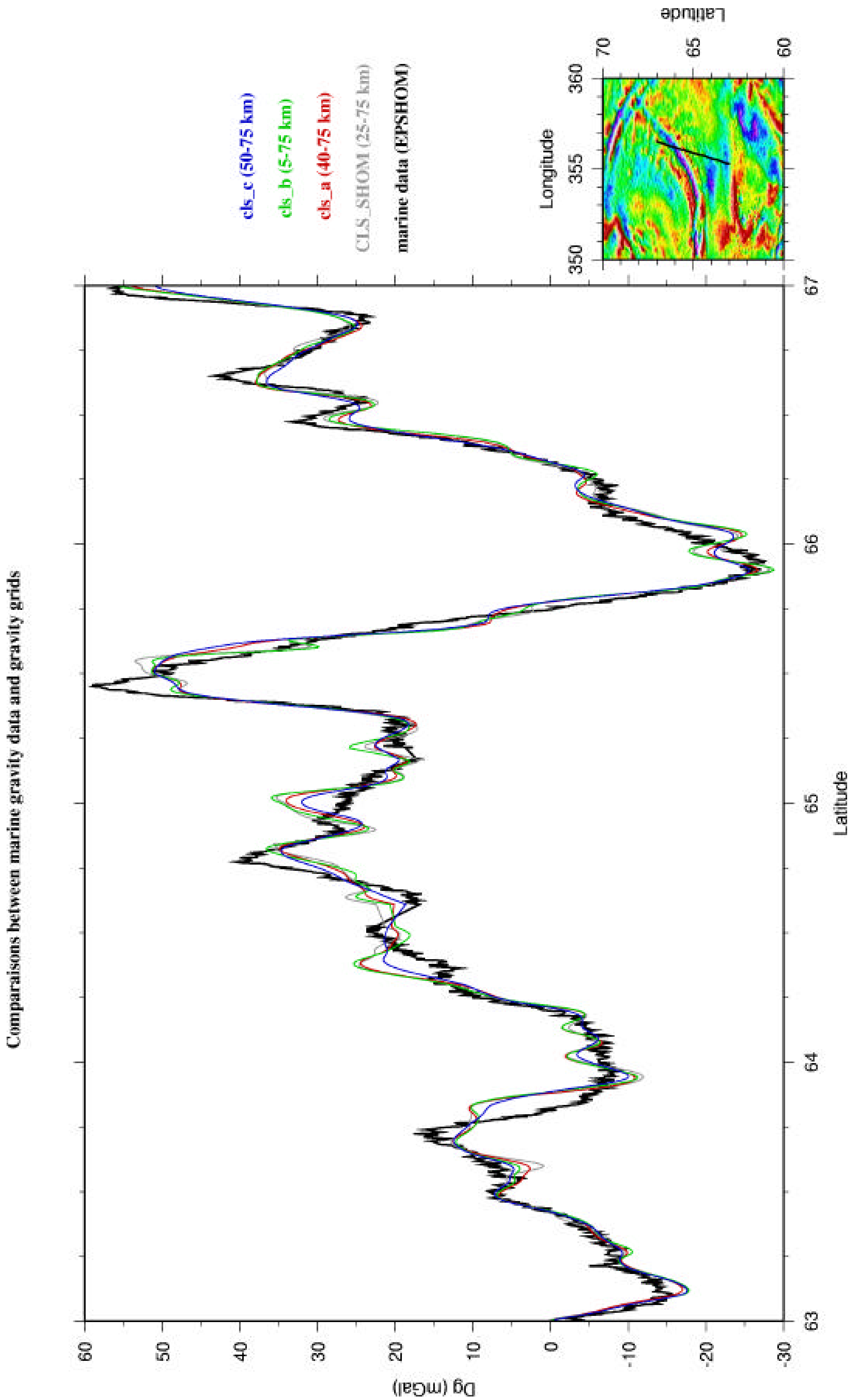

Figure 20: Comparisons between the marine gravity data (black) and the different determination of the CLS_SHOM99 GAS (see the text) along leg 2 (in mgal). The position of the leg is represented in black on the right lower side map.